

NBP-91-69

Sediment Erodibility In Narragansett Bay, RI: A Method of

Predicting Sediment Dynamics 58 pp

Keith, Davis, Paul (EPA-ERLN)

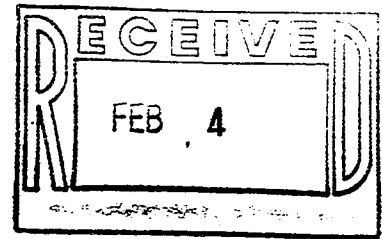
Narragansett Bay Estuary Program

**Sediment Erodibility In Narragansett Bay,
Rhode Island: A Method Of Predicting
Sediment Dynamics**

**Darryl J. Keith
Computer Sciences Corporation
EPA/ERLN**

**Wayne R. Davis
John F. Paul
EPA/ERLN**

#NBP-91-69



FINAL REPORT
OF THE
PROJECT ENTITLED:

SEDIMENT ERODIBILITY
IN
NARRAGANSETT BAY, RHODE ISLAND;
A METHOD OF PREDICTING SEDIMENT
DYNAMICS

BY

DARRYL J. KEITH¹
COMPUTER SCIENCES CORPORATION
EPA/ENVIRONMENTAL RESEARCH LABORATORY
NARRAGANSETT, RHODE ISLAND

WAYNE R. DAVIS AND JOHN F. PAUL
U.S. ENVIRONMENTAL PROTECTION AGENCY
ENVIRONMENTAL RESEARCH LABORATORY
NARRAGANSETT, RHODE ISLAND

PREPARED FOR
U.S. ENVIRONMENTAL PROTECTION AGENCY
REGION 1

¹new address: U.S. ENVIRONMENTAL PROTECTION AGENCY
ENVIRONMENTAL RESEARCH LABORATORY
NARRAGANSETT, RHODE ISLAND

ERL N Contribution No. 1112

FOREWORD

The United States Congress created the National Estuary Program in 1984, citing its concern for the "health and ecological integrity" of the nation's estuaries and estuarine resources. Narragansett Bay was selected for inclusion in the National Estuary Program in 1984, and the Narragansett Bay Project (NBP) was established in 1985. Narragansett Bay was designated an "estuary of national significance" in 1988. Under the joint sponsorship of the U.S. Environmental Protection Agency and the Rhode Island Department of Environmental Management, the NBP's mandate is to direct a program of research and planning focussed on managing Narragansett Bay and its resources for future generations.

The NBP will develop a draft Comprehensive Conservation and Management Plan (CCMP) by December, 1991, which will recommend actions to improve and protect the Bay and its natural resources.

The NBP has established the following seven priority issues for Narragansett Bay:

- management of fisheries
- nutrients and potential for eutrophication
- impacts of toxic contaminants
- health and abundance of living resources
- health risk to consumers of contaminated seafood
- land-based impacts on water quality
- recreational uses

The NBP is taking an ecosystem/watershed approach to address these problems and has funded research that will help to improve our understanding of various aspects of these priority problems. The Project is also working to expand and coordinate existing programs among federal, state and local agencies, as well as with academic researchers, in order to apply research findings to the practical needs of managing the Bay and improving the environmental quality of its watershed.

This report represents the technical results of an investigation performed for the Narragansett Bay Project. The information in this document has been funded wholly or in part by the United States Environmental Protection Agency through Cooperative Agreement #CX812768 to the Rhode Island Department of Environmental Management. It has been subject to the Agency's and the Narragansett Bay Project's peer and administrative review and has been accepted for publication as a technical report by the Management Committee of the Narragansett Bay Project. The results and conclusions contained herein are those of the author(s), and do not necessarily represent the views or recommendations of the NBP.

TABLE OF CONTENTS

DISCLAIMER	v
EXECUTIVE SUMMARY	vi
ABSTRACT	1
INTRODUCTION	1
PHYSICAL AND DEPOSITIONAL SETTINGS IN NARRAGANSETT BAY	2
METHODS	3
Sediment Sampling	3
Quantitative Analysis of Sediment Texture	4
Sediment Erodibility	5
Establishing Quantitative Relationships Between Shear Stress, Sediment Characteristics and Water Content	7
RESULTS	8
Sediment Erodibility	8
Water Content	9
Sediment Texture	9
Statistical Analyses	10
DISCUSSION	12
Potential Erodibility of Narragansett Bay Sediments	14
CONCLUSIONS	17
ACKNOWLEDGEMENTS	19
REFERENCES	20

LIST OF FIGURES

Figure 1. General map of the Narragansett Bay System.....	23
Figure 2. Sediment distribution in the Narragansett Bay System based on gravel, sand, silt and clay content.....	24
Figure 3. General map of sample locations	25
Figure 4. Textural classification of gravel-free sediments....	26
Figure 5. Range of Entrainment Rates for 2 dynes/cm ²	27
Figure 6. Range of Entrainment Rates for 3 dynes/cm ²	28
Figure 7. Range of Entrainment Rates for 4 dynes/cm ²	29
Figure 8. Range of Entrainment Rates for 5 dynes/cm ²	30

LIST OF TABLES

TABLE 1. Maximum Suspended Solids Concentration with Applied Shear	31
TABLE 2. Entrainment Rate at sample sites for each applied effective shear stress	33
TABLE 3. Percent water content for sediments at each of the sample sites	35
TABLE 4. Summary of sediment properties for sample sites	37
TABLE 5. Results of Method of Moments Calculations	39
TABLE 6. Summary of correlation analysis for samples sites from data obtained from Sediment Analyses	40
TABLE 7. Summary of Measured vs. Predicted entrainment rates for selected sample sites	42
TABLE 8. Summary of Measured vs. Predicted entrainment rates for all sample sites	43

LIST OF APPENDICES

APPENDIX I	Summary of Sediment Sampling Locations	44
APPENDIX II	Determination of Silt and Clay Content Using Pipette Analysis	45
APPENDIX III	Determination of Sand Content By Sieving	47
APPENDIX IV	Determination of Percent Water Content	48
APPENDIX V	Determination of Sediment Erodibility Using the Particle Entrainment Simulator (PES)	49

DISCLAIMER

This report has been reviewed by the Environmental Research Laboratory, U.S. Environmental Protection Agency, Narragansett, Rhode Island and approved for publication. Approval does not signify that the contents necessarily reflect the views and policies of the U.S. Environmental Protection Agency, nor does mention of trade names or commercial products constitute endorsement or recommendation for use.

EXECUTIVE SUMMARY

The overall objective of this one year investigation was to study the entrainment potential of Narragansett Bay sediments in the context of understanding coastal sediment transport processes.

The approach was to subject several sediment types in Narragansett Bay to a range of experimentally applied shear stresses and determine their erosiveness by developing quantitative relationships between shear stress, particle size data and water content. Statistical analyses of these variables resulted in first-order, polynomial equations which accounted for 70-90% of the variance in the data. These models were then used to calculate entrainment rates at shear stress levels of 2-5 dynes/cm². Based on the entrainment data, maps of sediment distribution along Narragansett Bay were transformed into maps of resuspension potential. Intended applications for these maps include the identification of areas that are suitable for sediment disposal (e.g. dredge spoil) based on dispersive or non-dispersive disposal strategies and to provide information on the potential transport of chemically-bound sediments relative to sediment lithology.

While developmental in nature, the models consistently identify areas within Narragansett Bay that have the highest and lowest potential for erodibility over the range of applied shear stresses. Generally, the most easily erodible sediments are located in the upper Narragansett Bay, along the Providence River, the Bristol Harbor area, and in Mount Hope Bay. These areas are characterized by fine grained sediments (e.g. silty clays and clayey silts) with high water contents. In comparison, the sediments with the lowest potential for resuspension occur at the entrances to Narragansett Bay and Greenwich Bay. These areas are characterized by sands with low water contents. The resuspension potential for the remainder of Narragansett Bay sediments increases as the percentages of silts, clays, and water contents increase.

The long-term recommendation from this investigation is that in situ measurements of shear stress and entrainment should be collected at several locations within Narragansett Bay, over a range of time scales. The establishment of this database would allow for comparisons with the simulated shear stresses and entrainment rates used in this study and form the cornerstone for an effective managerial scheme when merged with previously collected databases (e.g. bathymetry, sediment chemistry).

ABSTRACT

The objective of this study was to characterize the erodibility of surficial sediments of Narragansett Bay and quantitatively identify sedimentologic variables which affect erodibility. This objective was accomplished by: 1) quantifying the sediment textures that characterize Narragansett Bay; 2) measuring the resuspension potential of these sediments, as a function of experimentally applied shear stress; 3) establishing quantitative relationships between shear stress, sediment grain size and sediment water content; and 4) extrapolating the results of the empirical models to an existing map of sediment distribution for Narragansett Bay.

As expected, the most easily erodible sediments are those containing high percentages of fine material (i.e. silts and clays) and water contents (e.g. sections of the Providence River Dredge Channel, the Bristol Harbor area, and Mt. Hope Bay). Sediments with the lowest potential for resuspension are those containing high sand and low water contents (e.g. entrances to East, West and Sakonnet River Passages and the entrance to Greenwich Bay) or finer-grained sediments intermixed with mussel beds or overlain by amphipod mats. The potential erodibility for the remainder of Narragansett Bay sediments increases as the percentages of silts, clays and water contents increase.

INTRODUCTION

Estuarine sediments are a major reservoir of toxic chemicals which affects the near field exposure of both benthic and water column biota. The ability to model and predict the erodibility of these sediments is particularly important in determining the fate of contaminants such as nutrients, heavy metals, and toxic chlorinated hydrocarbons which enter readily adsorb onto silts and clays which can then be deposited along the seabed.

The objectives of this study are to: 1) examine textural and lithologic features that characterize the sediments of the

Narragansett Bay system; 2) determine the potential erodibility of these sediments, as a function of experimentally applied shear; 3) establish quantitative relationships between shear stress, sedimentary characteristics (e.g. size distribution, mean grain size, sorting) and sediment water content; and 4) compare the results of these relationships with a map of sediment distribution for Narragansett Bay.

Physical and Depositional Settings of Narragansett Bay

Narragansett Bay is a complex depositional environment characterized by gravels, sands, silts and clays deposited as a result of Holocene (~ 10,000 years before present) glacial and post-glacial fluvial, subaerial, estuarine, and marine processes. The most abundant sediments in the system are clayey silts and combinations of sands, silts, and clays. Sands are locally important (McMaster, 1960). The Narragansett Bay system consists of Narragansett Bay proper, Greenwich Bay, Mt. Hope Bay, and Sakonnet River Passage (Figure 1). Narragansett Bay proper is connected to Rhode Island Sound by two main passages: East Passage and West Passage. Mt. Hope Bay is connected to Rhode Island Sound by Sakonnet River Passage (Figure 1). Water depths within the Narragansett Bay system are generally less than 9 meters. However, along East Passage, the lower reaches of West Passage and Sakonnet River, water depths are in excess of 9 meters.

Previous sedimentary investigations of Narragansett Bay have

characterized bay sediments in terms of the percentages of sand, silt and clay content, areal distribution, petrography (McMaster, 1960; 1962; McMaster and Clarke, 1956; McMaster et al., 1956) and have modeled the seasonal deposition and net sediment transport rates of suspended material (Morton, 1972; Collins, 1974) along its main passages. Other studies have investigated the seasonal variability in compactness of sediments along the upper reaches of West Passage (McMaster, 1967), or examined the resuspension and depositional behavior of suspended material along West Passage (Oviatt and Nixon, 1975), and addressed the pollution history of the upper bay, south of the Providence River, as recorded in the sedimentary record (Goldberg et al., 1977).

METHODS

Sediment Sampling

Field programs were conducted during November 21-28, 1988 and June 13-17, 1989 onboard USEPA Ocean Survey Vessel PETER W. ANDERSON. These field programs collected samples from twenty-four sites in Narragansett Bay (Figure 3) which included eight of the twelve sediment classifications for Narragansett Bay and Rhode Island Sound. (McMaster, 1960; Figure 2). Rock outcrops, gravel and sandy gravel could not be sampled. Concentrations of gravel-silt-clay were not found in our study areas and were not sampled.

At each station, surficial sediments were collected by Smith-McIntyre grab and box coring techniques for site

characterization. The grab samples were photographed to provide a visual record of the station, color-classified using values and hues tabulated in the Geological Society of America Rock Color Chart (1984), subsampled for grain size and for sediment erodibility experiments. The box cores were subsampled for water content determination using 30.5 cm long sections of 8.9 cm diameter plexiglas coring tubing which were capped and sealed.

A summary of the sediment sampling locations is found in Appendix I.

The cores for the erodibility analysis were collected by partially inserting acrylic tubes (8.9 cm diameter) into the grab sample. The coring tubes were inserted to obtain surficial material, avoiding edges of the grab and any visible disturbance resulting from the sampling technique. These cores were then attached to a shipboard circulating seawater system to maintain sample integrity.

Quantitative Analysis of Sediment Texture

Standard pipette and sieve analyses were used to determine basic lithologic characteristics. Pipette analysis, based on particle settling velocity, is a widely used, highly reproducible technique for the determination of grain sizes less than 0.063 mm (4.0 phi). The methodology is summarized in Appendix II.

The greater than 0.063 mm (<4 phi) size fraction of the sediment samples was analyzed by sieve analysis. Sediments used in this analysis were sieved at 0.01 mm (0.5 phi) intervals between 1.4 and 0.063 mm (-0.5 phi to 4.0 phi). The methodology is

summarized in Appendix III.

Textural classifications were determined after methods developed by Folk et al. (1974). The sand, silt and clay contents for each sample station, as determined from the pipette and sieve analyses, were plotted on a ternary diagram to indicate textural class (Figure 6).

Mean grain size, sorting, skewness and kurtosis were determined using methods of moments calculations (Table 5). The method of moments is a mathematical technique that uses the individual weight percentages of the various size classes to determine the above variables. The major advantages of using this technique are the speed of analysis and freedom from the fundamental assumption that the sediments have lognormal size distributions (Blatt, Middleton and Murray, 1972 and Lewis, 1984). The values for sorting, skewness and kurtosis were interpreted according to the scales used in Folk and Ward (1957).

The water content of the surficial sediments at each site was determined from the saturation content. Saturation content is expressed as the percent of the total sediment weight which contains water. The methodology is summarized in Appendix IV.

Sediment Erodibility

The sediment cores were subjected to experimentally applied shear stresses using the Particle Entrainment Simulator (PES). The PES is a portable device designed for the rapid measurement of sediment resuspension from relatively undisturbed sediment samples (Lavelle

and Davis, 1987). The amount of material resuspended is related to the effective shear stress which is proportional to the frequency of oscillation (Tsai and Lick, 1986). A more complete description of the PES is summarized in Appendix V.

Four oscillation rates were applied to the Narragansett Bay sediment samples, i.e. 4 shear stresses were applied. These rates are 0.16, 0.12, 0.10 and 0.08 seconds/cycle, which correspond to equivalent shear stresses of 2, 3, 4, and 5 dynes/cm² (Tsai and Lick, 1986). Lavelle and Davis (1987) indicate that, while the turbulence field generated by the PES differs from that generated by a horizontal shear flow, it is the presence of instantaneous turbulent stresses in the boundary layer of both types of flow that create conditions which result in resuspension of deposited material.

At each applied shear stress aliquots of suspended material were withdrawn from the core at regular time intervals, turbidity (the percentage of light attenuated) was determined for the subsample by light transmissometry, and the slurry returned in order to conserve volume and material. The turbidity of the samples was measured at a wavelength of 660 nm using a Bausch and Lomb Spec 20 spectrophotometer.

The entrainment of material (the movement of sediment from the bed into suspension) was monitored over time until an equilibrium concentration, as determined by consistent turbidity values, was reached (Appendix V). In some cases this took more than 35 minutes to achieve.

The light attenuation data were then used to empirically derive (from Davis, unpublished data) a formula which determines suspended solids concentration (mg/l) for each level of shear stress over the duration of the experiment (Appendix V).

Establishing Quantitative Relationships Between Shear Stress, Sediment Characteristics and Water Content

Laboratory experiments (Partheniades, 1965; Mehta and Partheniades, 1975; Fukuda and Lick, 1980; Lee et al., 1981 and Lick, 1982) have indicated that entrainment is dependent on several parameters such as shear stress, water content, particle size distribution, mineralogy, and the effects of benthic organisms. By using statistical correlation and regression techniques, we have quantitatively related applied shear stress to water content and particle size distribution.

The generation of these relationships occurred in a two-step process. Initially, a subset of the data (fifteen of the twenty-four sites) was used to determine which sedimentary parameters showed correlations with the measured entrainment rates. These parameters were determined using the Pearson product-moment correlation statistic, which measures the closeness of a linear relationship between two variables. This relationship and its statistical significance was then used to determine whether a parameter was to be kept or excluded from further consideration. During this study the statistical significance was $\alpha = 0.05$.

Linear regression techniques were then applied (to those

sediment properties showing correlations with the measured entrainment values) to produce numerical equations that could act as surrogate predictors. The numerical models selected for use in the erodibility analysis were those whose combination of sediment properties resulted in the largest R^2 value (i.e. the combination which accounted for the largest percentage of the variance in the data) and contained the smallest number of inputs (i.e. requires a minimal number of measurements).

The data produced by these "test" models were then subjected to an analysis of variance using least-squares estimates for comparisons with measured entrainment values.

RESULTS

Sediment Erodibility

The maximum amount of material resuspended as a function of shear stress at each site is summarized in Table 1. Examination of these data indicate that a range of suspended solids concentrations and equilibrium times are created with varying levels of shear stress. These data further indicate, as expected, that as shear stress increases there is corresponding increase in amounts of suspended material entrained into the water column and that longer times are required before equilibrium conditions are reached. Finally, there is a direct correlation between the amount of material placed in suspension at the various shear stresses and sediment type.

An examination of entrainment rate for the range of shear

stresses (Table 2) indicates that entrainment did not behave in a linear fashion at the sediment stations but did produce a general agreement that increased shear yields increased entrainment.

Water Content

Water content of the surficial sediments at the sampling sites varies considerably from less than 20% to greater than 80% and differs in response to sediment type and location in the bay system (Table 3).

Sediment Texture

Narragansett Bay can be described as containing extremely poorly sorted, very poorly sorted, and poorly sorted sediments (Table 5). Further, these sediments can be classified into six of the ten textural classes for gravel-free detrital sediments (Figure 6) proposed by Folk et al. (1970). Silty sand and sandy silt were the most commonly occurring textures and appear to characterize a significant portion of lower and upper Narragansett Bay (Figure 2; McMaster, 1960). The remainder of the sample sites contain gradations of sand (i.e. sand, muddy sand, and sandy mud) and silt. The results of these analyses are in agreement with those of MacMaster (1960) and continue to substantiate the validity of that dataset for the sediment distribution of Narragansett Bay. The sediment textural properties as determined by field, laboratory and statistical analyses are summarized in Tables 4 and 5.

Statistical Analyses

The results of the correlation analysis indicated that there were associations between measured entrainment values and 11 of the 15 sediment parameters (Table 6). Statistically significant associations were found with mean and median grain size, variance, standard deviation, skewness, sorting, mode, % sand, % silt, % clay and % water. Regression analyses resulted in mathematical expressions which accounted for 76-87% of the variance within the dataset. This is notable as these models do not consider the variance introduced due to sampling design or analytical technique used. The numerical equations for the various levels of shear stress are:

$$\begin{aligned} \text{ERATE2} = & 0.07182 + 0.03331(\text{MNGR}) - 0.03364(\text{MEDGR}) + 0.01095(\text{VAR}) - \\ & 0.05935(\text{SORT}) + 0.00642(\text{MODE}) - 0.00119(\text{PSILT}) - \\ & 0.00074(\text{PWATER}). \end{aligned}$$

$$R^2 = .758$$

where ERATE2= predicted entrainment rate at
a shear stress of 2 dynes/cm²,
MNGR= mean grain size,
MEDGR= median grain size,
VAR= variance,
SORT= sorting,
MODE= mode,
PSILT= % silt,
PWATER= % water.

$$\begin{aligned} \text{ERATE3} = & -0.05394 - 0.02012(\text{MEDGR}) + 0.00964(\text{VAR}) - \\ & 0.03207(\text{SORT}) + 0.01096(\text{MODE}) + 0.00101(\text{PSAND}) - \\ & 0.00061(\text{PWATER}). \end{aligned}$$

$$R^2 = .711$$

where ERATE3= predicted entrainment rate at a shear stress of
3 dynes/cm².

$$\begin{aligned} \text{ERATE4} = & 0.05899 + 0.00755(\text{MNGR}) - 0.01506(\text{MEDGR}) + 0.01122(\text{VAR}) - \\ & 0.04446(\text{SORT}) + 0.00541(\text{MODE}) - 0.00186(\text{PSILT}) - \\ & 0.00063(\text{PWATER}). \end{aligned}$$

$$R^2 = .870$$

where ERATE4= predicted entrainment rate at a shear stress of 4 dynes/cm².

$$\begin{aligned} \text{ERATE5} = & 0.3492 + 0.14128(\text{MNGR}) - 0.09617(\text{MEDGR}) + 0.05324(\text{VAR}) - \\ & 0.28124(\text{SORT}) - 0.00793(\text{PSILT}) - 0.00399(\text{PWATER}). \end{aligned}$$

$$R^2 = .778$$

where ERATE5= predicted entrainment rate at a shear stress of 5 dynes/cm².

Least squares analysis of the measured vs. the predicted entrainment values for the "test" subset produced results that are in general agreement (Table 7). This is to be expected as the equations produced are derived from the data but are indeed very interesting since these results are based solely on sediment characteristics and ignore the effects of other factors (e.g. animal-sediment interactions).

A comparison of the measured vs. the predicted entrainment values for the full dataset suggests that the derived numerical models do reasonably reproduce values similar to those measured experimentally (Table 8).

DISCUSSION

The results in Table 8 indicate that for several stations the predicted entrainment rates are higher than the measured entrainment rates. Even so, the models consistently predict, at all levels of shear, low erodibility for those sites characterized by coarse sediments and low water contents and high erodibility for those fine-grained areas with high water contents (Table 8). The discrepancies are possibly related to the effect that biological parameters (e.g. species type, species density or diversity) may have on erodibility. These factors were not taken into account during the development of the numerical models.

According to Davis and Means (1986) and Davis et al. (in review), deposit-feeding organisms (in particular, the bivalves Nucula annulata and Yoldia limatula) can increase entrainment rate two-four fold. This increase is the result of the destabilization of the sediment surface by changing the sediment water content and boundary roughness as the bivalves burrow through cohesive sediments (Davis and Means, 1986). During this process, upper layer sediments become more viscous as the extension of bivalve siphons fracture the cohesiveness of the sediment matrix adjacent to each individual during subsurface locomotive activities. Consequently, as time and burrowing increase, the upper sediment surface (0-4 mm) becomes very unconsolidated relative to the underlying sediments.

The increase in entrainment was also found to be proportional to bivalve abundance and time of working. Bender and Davis (1984)

estimate typical densities of Yoldia to 100-300 bivalves/m² in Narragansett Bay. These densities suggest that these species have the ability to significantly alter the entrainment rates of sediments through their daily activities. Davis et al. (in review) indicate that during their experiments, there was no effect by Nucula on entrainment at 2 dynes/cm². However, the effect began to become increasingly evident at 3, 4, and 5 dynes/cm².

Field descriptions for sites 2, 4, 8, 9, 10, 12, 19, and 23 indicate that sediments at these locations contain species of bivalves and polychaete worms. The entrainment rates calculated from the PES data are generally higher at 3, 4, and 5 dynes/cm² than those predicted by the models (see Table 8), with the largest differences occurring at the 5 dyne/cm² shear stress level. This difference may be explained by the observation of Davis et al. (in review) that moderate abundances in Nucula may increase resuspension during high shear periods (e.g. 5 dynes/cm²). Therefore, the underprediction of entrainment by the models may be linked to biological alteration of the sediments.

The activities of other benthic organisms may also act to decrease particle entrainment through the stabilization of sediments by the release of compounds which bind particles, by growing roots and constructing tubes or by the formation of mats (Davis et al., in review). This theory is also supported by the PES measurements conducted during our study.

Field descriptions of sites 6, 11, 13, and 18 indicate that the surficial sediments contained species of Ampelisca, a mat-

former. Sediments at Site 18 were overlain by a dense mat of *Ampelisca*. At these sites, the calculated entrainment rates were generally lower than those predicted by the models. At 2 dynes/cm², the calculated rates were three to eight times lower than those rates predicted solely on sedimentary parameters. At 5 dynes/cm², the calculated rates were two to three times lower than the predicted rates. These differences suggest that the alteration of the substrate by the mat-forming processes of *Ampelisca* sp. significantly changed the potential erodibility of the surficial sediments.

The models over-predict entrainment values at sites 1, 6, 11, 13, 16, 18, 20, 21, 22, and 24. The common link to these sites are the presence of *Ampelisca*, bivalves and amphipod tubes which have acted to change the substrate by forming mats and binding sediments during the tube building process.

These data indicate, as suggested by Davis et al. (in review), that a quantitative description of entrainment should incorporate biological influences in addition to those imposed by physical processes and sedimentological properties.

Potential Erodibility of Narragansett Bay Sediments

The calculated values of entrainment were plotted versus sediment type for Narragansett Bay in order to estimate the potential for resuspension of bay sediments over a range of shear stresses. This simulation did not take into account the realities

that due to water depth or ambient current regime, these sediments may or may not experience the range of shear stresses used in this study.

At two dynes/cm² (Figure 5) the potential for resuspension appears to be the lowest from Prudence Island south along East and West Passages and from the head to the mouth of Sakonnet River Passage. The potential for highest erodibility is in the Upper Bay region and in Mt. Hope Bay. This distribution is not surprising given the general decrease in grain size from the Lower Bay to the Upper Bay. The very lowest rates of entrainment (i.e. the least erodible sediments) generally occur at the entrances to East, West, and Sakonnet River Passages; at the entrance to Greenwich Bay, east of Rome Point (West Passage); and along Warwick Pt. These sites correspond to areas with the high sand content (65-98%), low silt (4-25%), low clay (0-10%) and low water contents (18-24%).

Sediments become more erodible from Fort Adams (East Passage), north to the middle of Prudence Island and east into the entrance to Mt. Hope Bay in East Passage and from Rome Pt., north to Prudence Island (West Passage). This increase in erodibility is attributed to a rise in water contents (ranges from 38-55%), silt (35-52%), and clay (5-13%) concentrations relative to a decreasing sand content (36-60%). Sediments in this area range from silty sands and sandy silts to clayey silts.

Due to a further increase in the silt (50-70%) and clay (19-32%) content and water content (50-80%), the most easily erodible sediments, at this shear stress, occur in the Bristol Harbor area,

at the mouth of the Warren River, near Calf Pasture Point (West Passage), along the middle to upper sections of Sakonnet River Passage, between Popasquash Neck and Prudence Island (Upper Bay), along the Providence River shipping channel and in Mt. Hope Bay. Sediments at these sites are primarily composed of fine-medium clayey silts.

Although situated near coarse sand and gravel deposits, an area immediately adjacent to Castle Hill (East Passage) also contains easily erodible sediments. This increase in erodibility may be attributed to the relatively high silt (19.7%) and clay content (13.7%) of the gravelly, fine sand which characterizes the area.

At three and four dynes/cm² (Figure 6 and Figure 7), the potential for resuspension and entrainment are again the lowest along the entrances to East, West and Sakonnet River passages. Again, the most erodible sediments occur in the Upper Bay, along Mt. Hope Bay and at Castle Hill. Entrainment rates increase along the lower portion of East Passage and between Quonset Point and Prudence Island.

The predictive results for a shear stress of five dynes/cm² (Figure 8) indicate that the lowest potential for entrainment again occurs in the areas with the highest sand contents (64-98%) and lowest water contents (15-20%) such as the entrances to East, West and Sakonnet Passages and at the entrance to Greenwich Bay. The most easily erodible sediments at this shear stress occur in the Upper Bay, along the Providence River dredge channel, along Mt. Hope Bay, in the Bristol Harbor area, at the entrance to Warren River, between

Popasquash Pt. and Prudence Island (Upper Bay), and at Castle Hill (East Passage). Sediments at these sites are characterized by clayey silts or contain high silt and clay contents, as in the case of Castle Hill.

CONCLUSIONS

Sediments were collected from twenty-four locations within Narragansett Bay. These sediments were analyzed for information on their textural properties and to determine their erodibility as a function of experimentally applied shear stress. The field results indicate that Narragansett Bay consists of several types of sediments with a variety of grain size distributions and textures. Sidescan sonar imagery of the seafloor at the sampling sites suggests that these areas are primarily areas of deposition, based on their morphological and sedimentological characteristics (McMaster, 1989). This suggestion is made due to the lack of diagnostic erosional features. However, this situation may change during the advent of extreme storm conditions. Areas of active sediment transport are found at the entrance to Sakonnet River Passage where large-scale sedimentary bedforms are found and at the entrance to West Passage where small-scale bedforms have been observed (R. McMaster, personal communication).

The experimental and statistical modeling results indicate that a wide range of entrainment rates are possible for the sediments of the bay. While the models are experimental in nature, they

consistently predict and identify areas in the Narragansett Bay system with highest and lowest erodibility potential. It is, however, difficult to determine how representative the determined entrainment rates are of the actual processes in the Bay. Direct in situ measurements of shear stress and entrainment (Bedford et al., 1988) on a range of time scales would give insight into which shear stresses approximate conditions in the study area. The exploratory modeling effort discussed in this report did not include the biological influences in the determination of entrainment rates. This process needs to be quantified and included in future modeling efforts.

ACKNOWLEDGEMENTS

This study was supported by EPA contract # 68-01-7365 and # 68-01-7176 with Computer Sciences Corporation. The authors wish to thank E. Dettmann and H. Walker (USEPA), J. Heltshe (Computer Sci. Corp.), W. Munns (Sci. Applications International Corp.), J. King and R. McMaster (URI) for their insight during data processing, model development and data interpretation and critical reviews of the manuscript. Thanks also to R. Tyce (URI) and M. Bothner, B. Irwin, D. Twichell and T. O'Brien (USGS-Woods Hole) for technical assistance; the officers and crew of the OSV PETER W. ANDERSON for their support and dedication during the field program; C. Karp (Narragansett Bay Project) and K. Kipp (EPA-Region 1) for their support during this study.

REFERENCES

- Bedford, K., O. Wai, C.M. Libick and R. Van Evra III, 1987. Sediment Entrainment and Deposition Measurements in Long Island Sound. Jour. of Hydraulic Eng., October, pg. 1325-1342.
- Bender, K. and W.R. Davis, 1984. The effect of feeding by Yoldia limatula on bioturbation. Ophelia, 23, vol 1, pg 91-100.
- Blatt, H., G. Middleton and R. Murray, 1972. Origin of Sedimentary Rocks. Prentice-Hall, Inc., Englewood Cliffs, N.J.
- Collins, Barclay P., 1974. Suspended Material Transport In Lower Narragansett Bay and Western Rhode Island Sound. M.S. Thesis, University of Rhode Island, 85 pg.
- Davis, W.R. and J.C. Means, 1986. A developing model of benthic-water contaminant transport in bioturbated sediment. Proceedings of the 21st European Marine Biology Symposium, Gdansk, Poland.
- Davis, Wayne R., Wayne R. Munns and John F. Paul, in review. An Experimental Study Of the Role Of Bioturbation In Sediment Resuspension.
- Folk, R.L., 1974. Petrology of Sedimentary Rocks, Hemphill, Austin, Tx., 129 p.
- Folk, R.L., Peter B. Andrews and D.W. Lewis, 1970. Detrital Sedimentary Rock Classification and Nomenclature for use in New Zealand. N.Z. Jour. Geol.Geophys., 13: 937-68.
- Folk, R.L. and W.C. Ward, 1957. Brazos River Bar: A Study in the significance of Grain Size Parameters. Journal of Sedimentary Petrology, volume 27, pp.3-27.
- Fukuda, M.K. and W. Lick, 1980. The entrainment of cohesive sediments in freshwater. Journal of Geophysical Research, 85:2813-2824.
- Geological Society of America, 1984. Rock-Color Chart. Prepared by the Rock-Color Chart Committee: E.N. Goddard, P.D. Trask, R.K. De Ford, O.N. Rove, J.T. Singewald, Jr. and R.M. Overbeck. Distributed by the Geol. Soc. of America, Boulder, Colorado.

- Goldberg, Edward D, Eric Gamble, John J. Griffin and Minoru Koide, 1977. Pollution History of Narragansett Bay as Recorded in its Sediments. Estuarine and Coastal Marine Science, 5, 549-561.
- Lavelle, J.W. and W.R. Davis, 1987. Measurements of Benthic Sediment Erodibility in Puget Sound, Washington, NOAA Technical Memorandum ERL PMEL-72.
- Lee, D.Y., W. Lick and S.W. Kang, 1981. The entrainment and deposition of fine-grained sediments in Lake Erie. Journal of Great Lakes Research, 7, p.264-275.
- Lewis, D.L., 1984. Practical Sedimentology, Hutchinson Ross Publishing Co., Stroudsburg, Penn., 229p.
- Lick, W., 1982. Entrainment, deposition and transport of fine-grained sediments in lakes. Hydrobiologia, v. 91, p. 31-40.
- McMaster, R.L. and Clarke, W.B., 1956. A Survey of Bottom Surface sediments in Upper Narragansett and Mt. Hope Bays, Reference No. 56-14, Report 1, Submitted to the Corps. of Engineers, U.S. Army, Office of the Division Engineer, New England Division, Contract No. DA-19-016-CIVENG-56-1071 (Modification 1), June, 6 p.
- McMaster, R.L., D.E. Frazier and R.E. Carr, 1956. A Survey of Bottom Surface Sediments in Lower Narragansett Bay, Reference No. 56-18, Report 2, Submitted to the Corps. of Engineers, U.S. Army, Contact No. DA-19-016-CIVENG-56-1071, New England Division, September, 12 p.
- McMaster, R.L., 1960. Sediments of Narragansett Bay System and Rhode Island Sound, Rhode Island, Jour. Sed. Petrology, Vol. 30, p. 249-274.
- McMaster, R.L., 1962. Petrography and Genesis of Recent Sediments in Narragansett Bay and Rhode Island Sound, R.I., Jour. Sed. Petrology, Vol. 32, No. 3., p. 484-501.
- McMaster, R.L., 1967. Compactness Variability of Estuarine Sediments: An In Situ Study. Estuaries., AAAS, pg 261-267.
- McMaster, R.L., 1984. Holocene Stratigraphy and Depositional History of the Narragansett Bay System, Rhode Island, USA, Sedimentology, Vol. 31, p 777-792.
- McMaster, R.L., 1989. Narragansett Bay Project Core Sites: Bottom Conditions Based Upon Bathymetric and Sidescan Sonar Surveys, Unpublished report.

- Mehta, A.J. and E. Parthenaides, 1975. An investigation of the depositional properties of flocculated fine sediments, J. Hydraulic Res., Vol. 13, p.361-381.
- Morton, Robert W., 1972. Spatial and Temporal Distribution of Suspended Sediment in Narragansett Bay and Rhode Island Sound. Geol. Soc. of Am. Memoir 133, p.131-141.
- Oviatt, Candace A. and Scott W. Nixon, 1975. Sediment Resuspension and Deposition in Narragansett Bay. Estuarine and Coastal Marine Science, 3, p. 201-217.
- Partheniades, E., 1965. Erosion and deposition of cohesive soils. J. Hydraulics Div. American Society of Civil Engineers, Vol. 91, (HY1) p. 105-139.
- Tsai, C-H. and Lick, W., 1986. A Portable Device for Measuring Sediment Resuspension, J. Great Lakes Res., Vol. 12, p. 314-321.

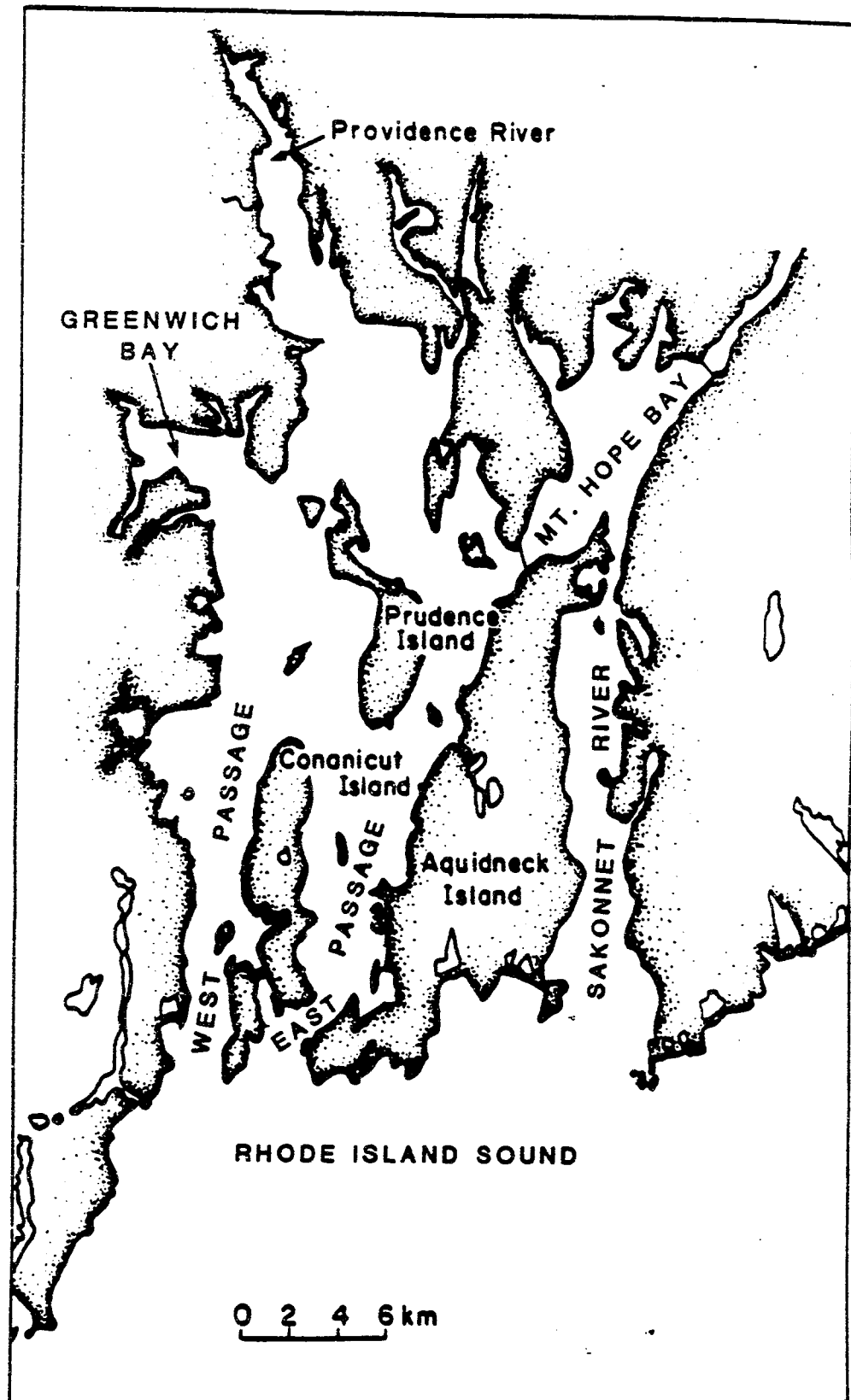


Figure 1. General location map of the Narragansett Bay System.

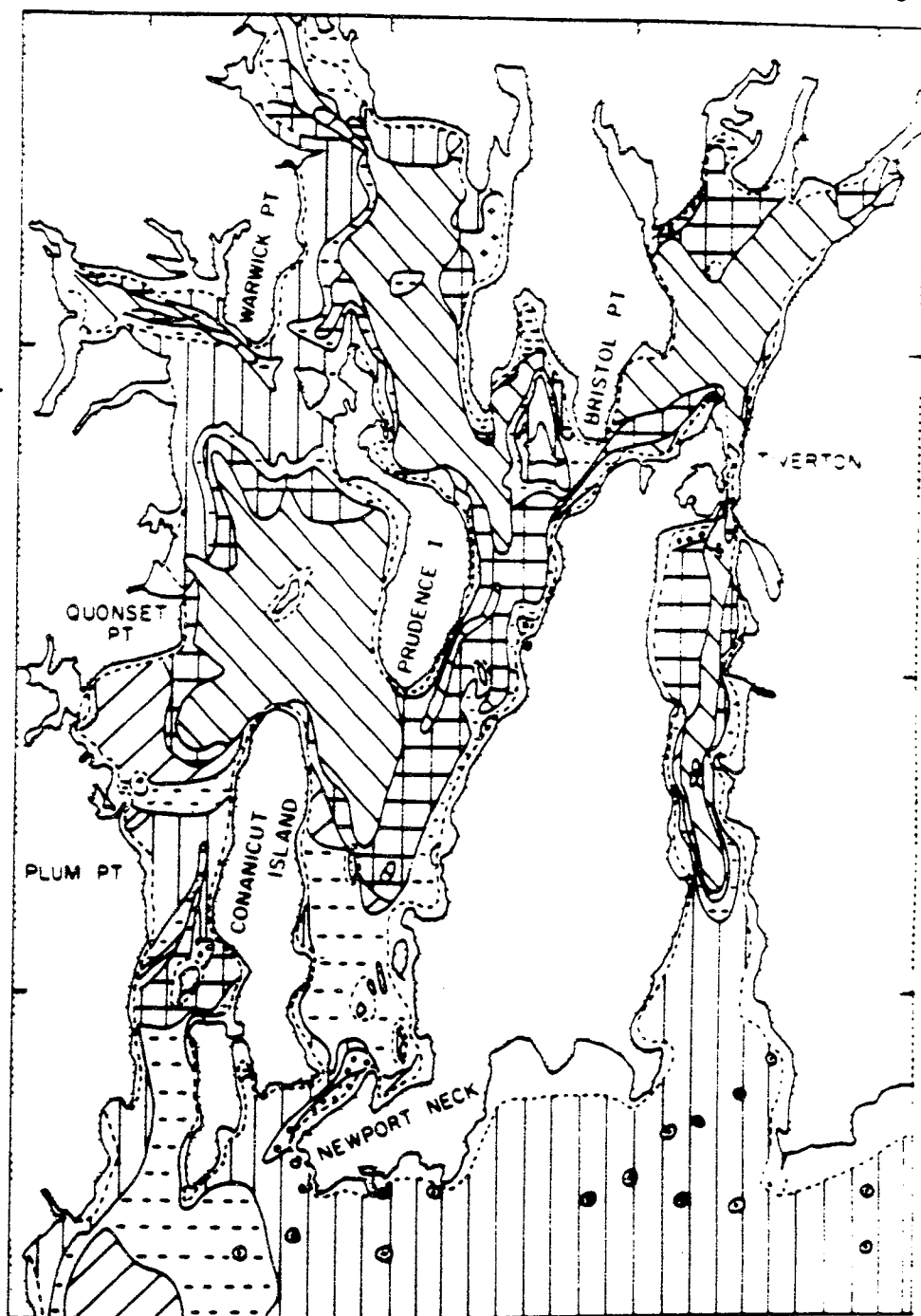
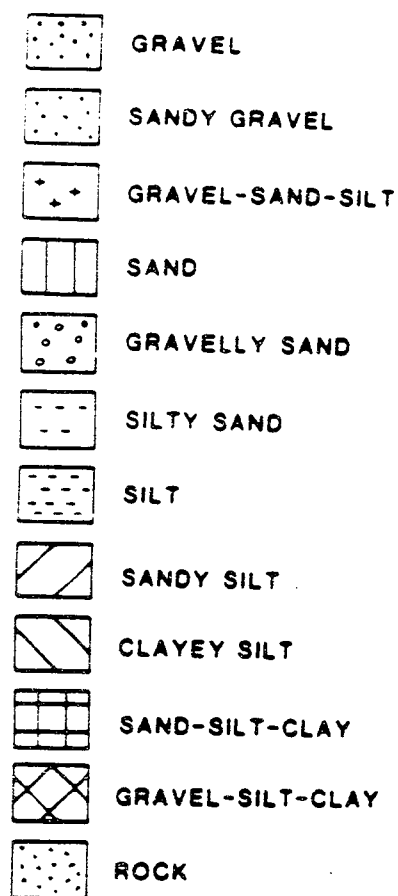


Figure 2. Sediment distribution in the Narragansett Bay System based on gravel, sand, silt and clay content (From McMaster, 1960).

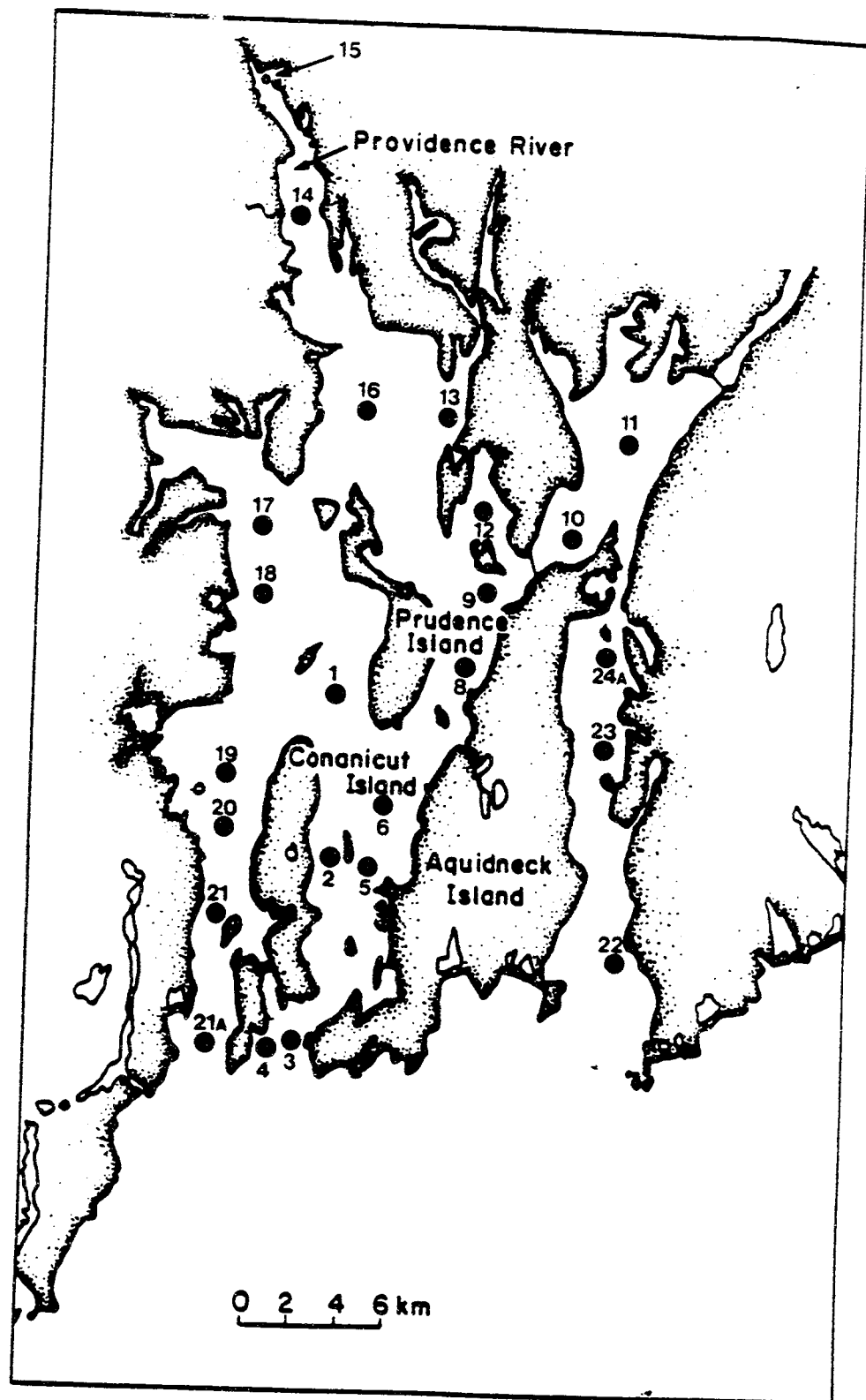


Figure 3. General map of sample locations.

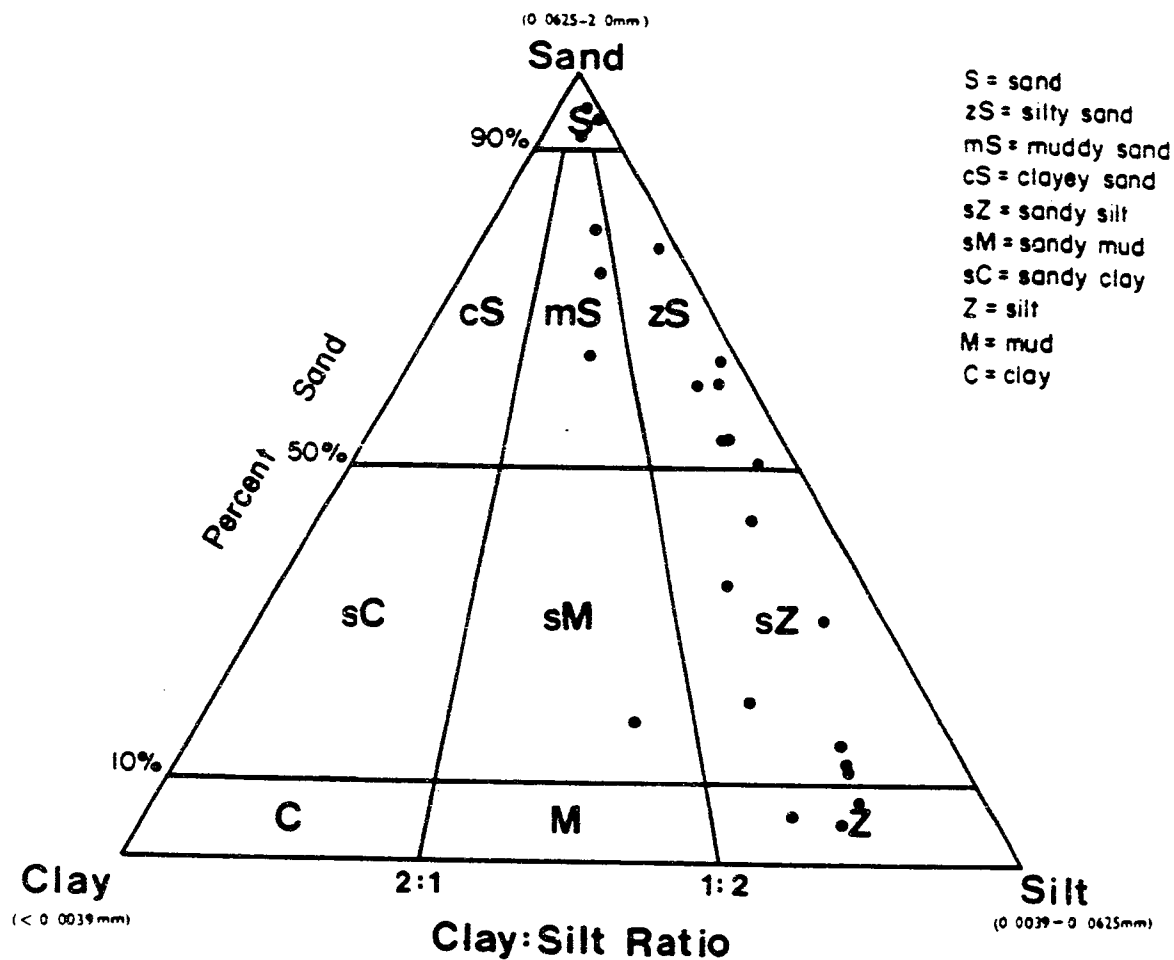


Figure 4. Textural classification of gravel-free sediments. Classes are defined by the percentage of sand and the ratio of clay to silt. Dots represent the distribution of Narragansett Bay sediments sampled during this study (Figure modified from Folk et al., 1974).

Figure 5. Range of entrainment rates for 2 dynes/cm² based on the distribution of sediment types of McMaster, 1960.

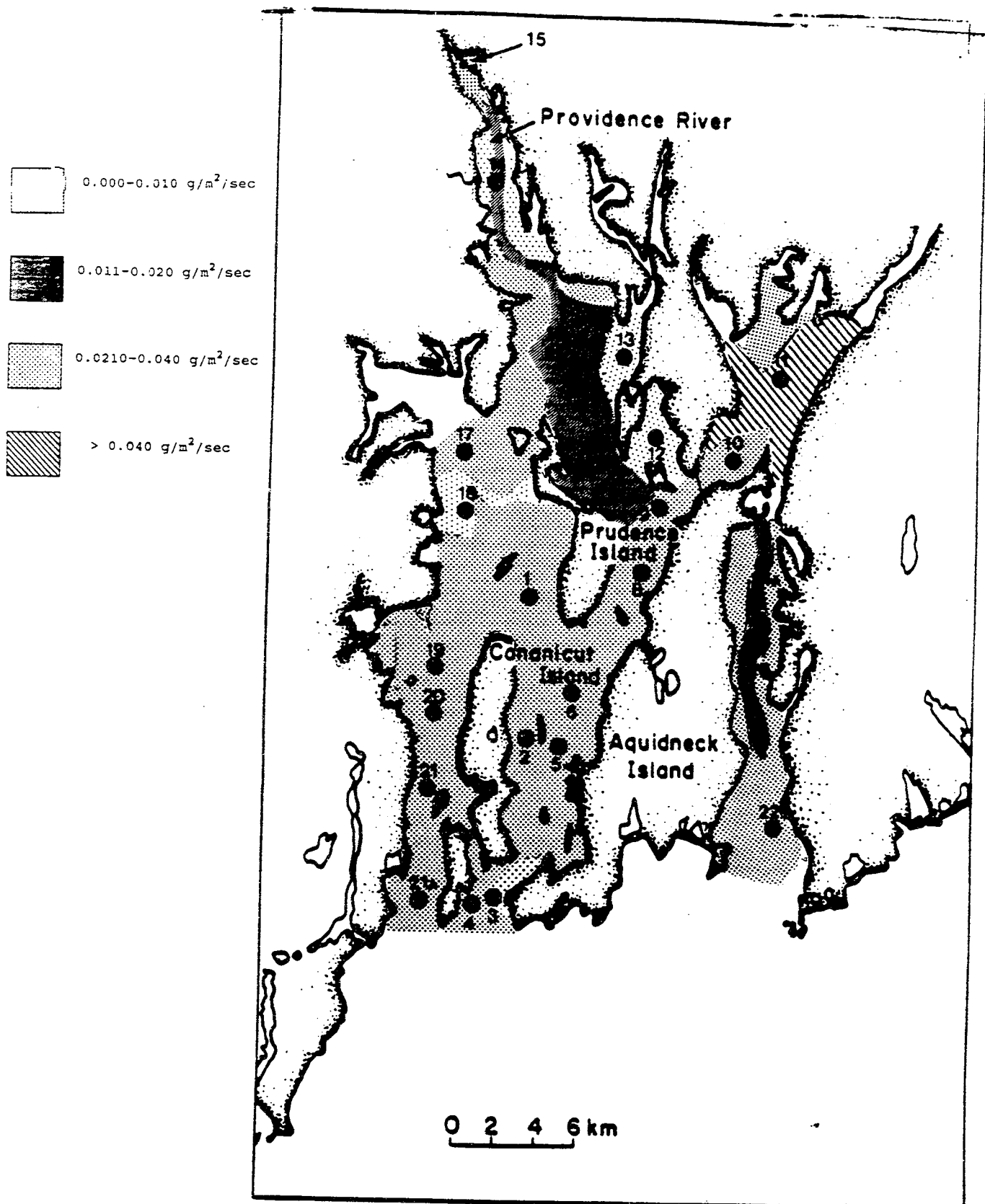


Figure 6. Range of entrainment rates for 3 dynes/cm² based on the distribution of sediment types of McMaster, 1960.

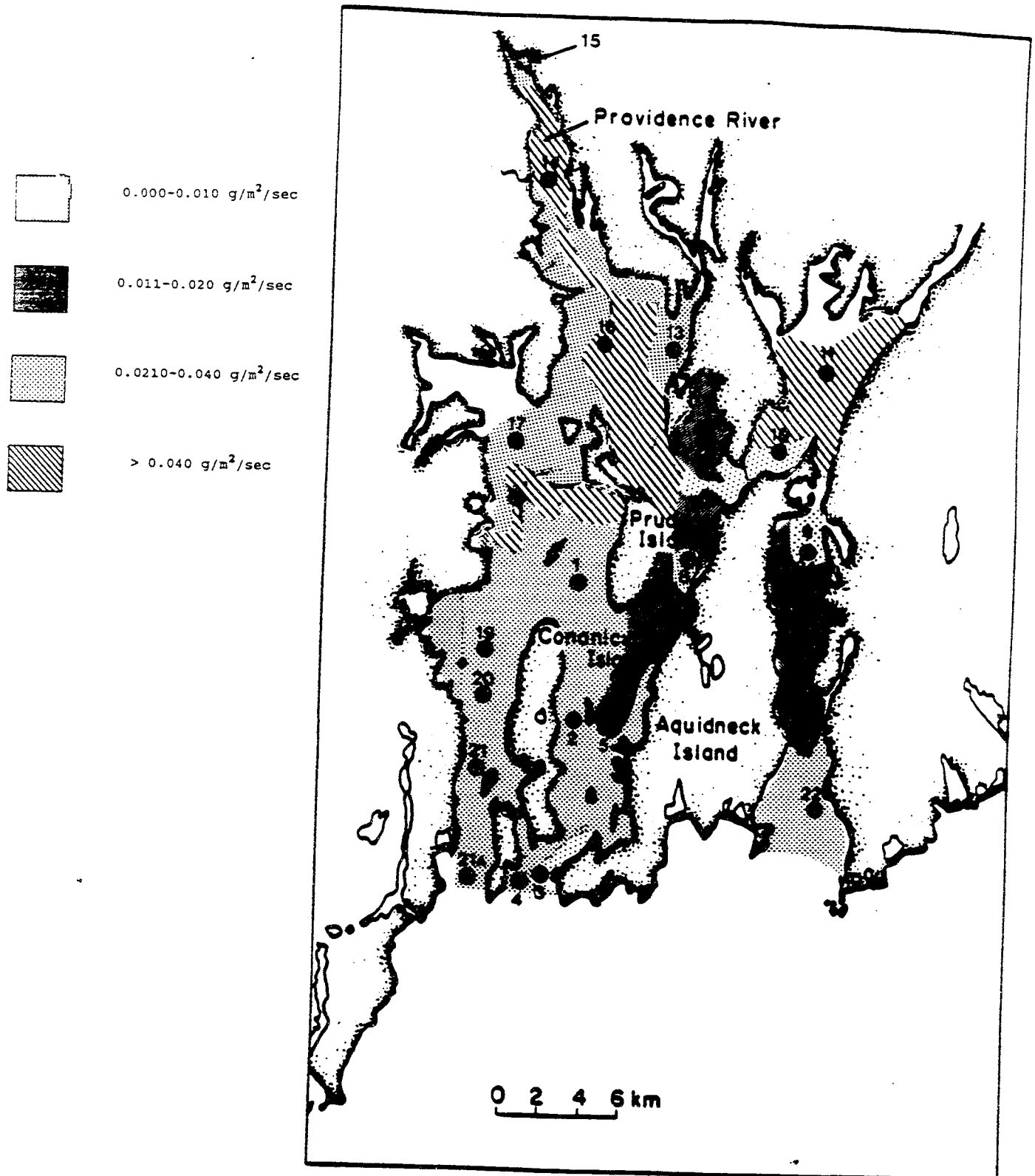


Figure 7. Range of entrainment rates for 4 dynes/cm² based on the distribution of sediment types of McMaster, 1960.

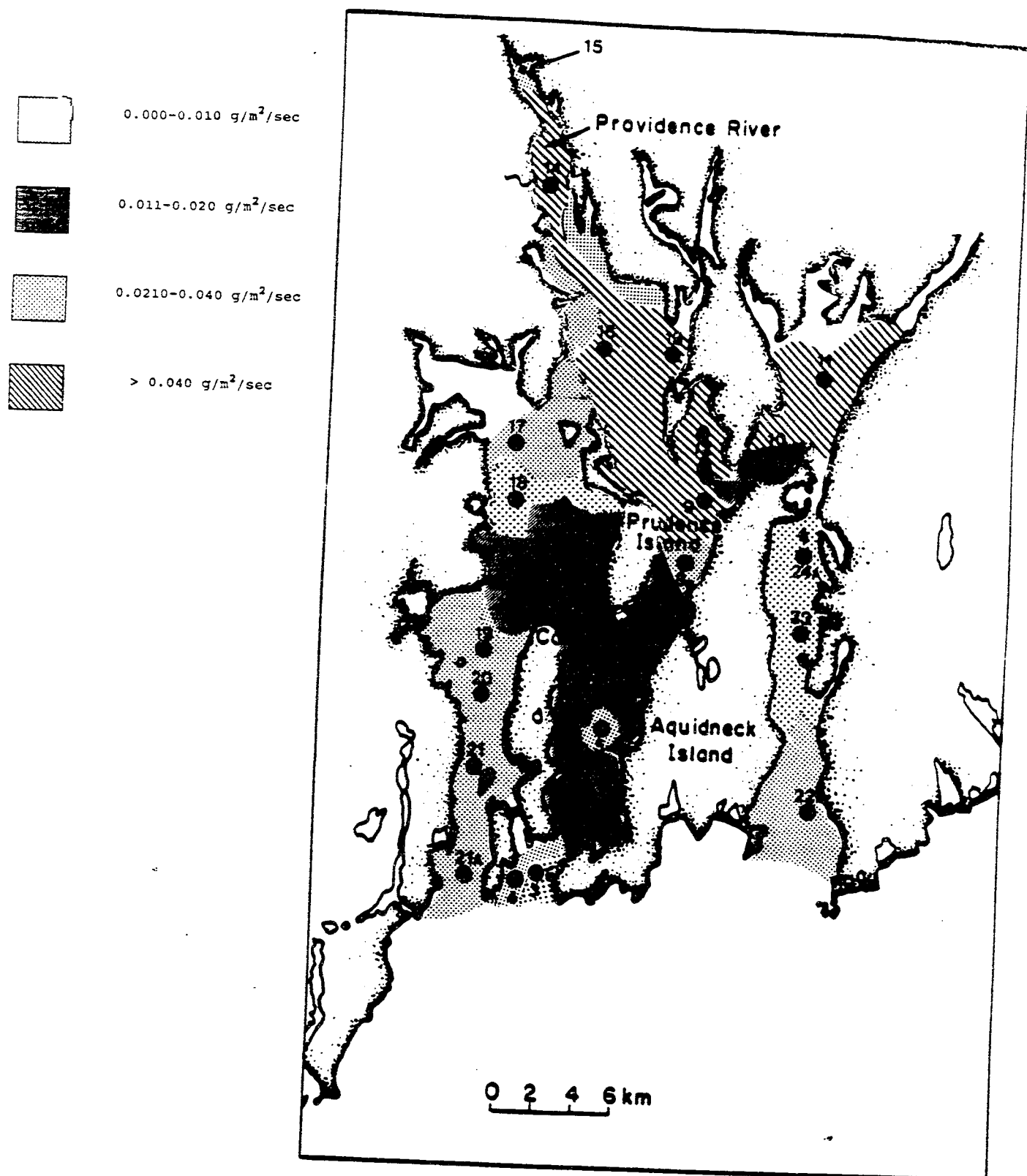


Figure 8. Range of entrainment rates for 5 dynes/cm² based on the distribution of sediment types of McMaster, 1960.

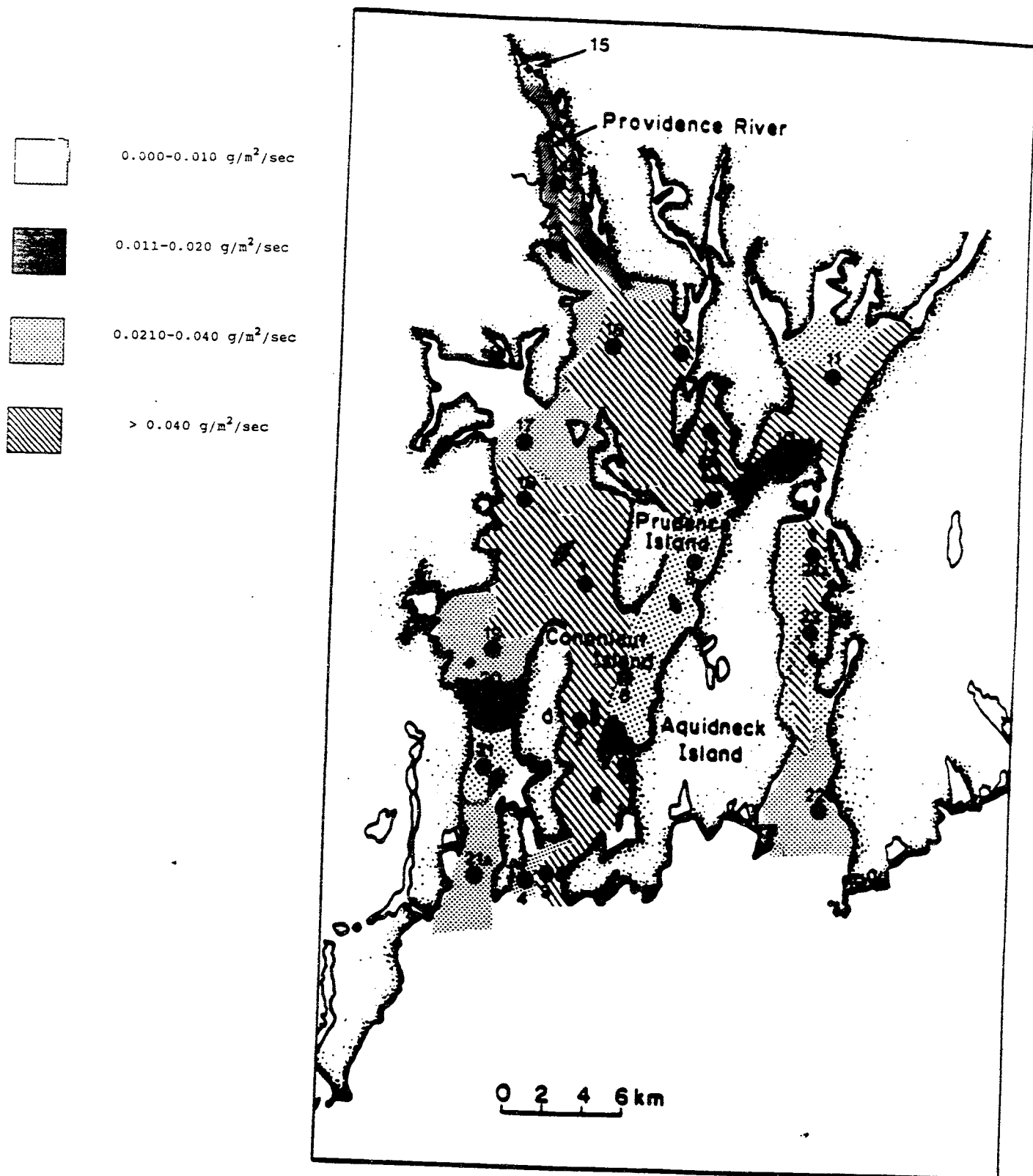


TABLE 1

MAXIMUM SUSPENDED SOLIDS CONCENTRATION WITH APPLIED SHEAR

STA.	TIME*	2 DYNE TEST	TIME	3 DYNE TEST	TIME	4 DYNE TEST	TIME	5 DYNE TEST
	(min)	(g/m ²)	(min)	(g/m ²)	(min)	(g/m ²)	(min)	(g/m ²)
1	15	9.49	30	27.57	35	33.58	40	139.95
2	20	13.18	25	38.13	25	26.55	25	106.84
4	10	2.29	15	8.10	20	11.47	30	42.53
5	15	14.47	35	26.82	50	59.59	40	82.59
6	10	1.04	10	10.17	25	22.47	35	74.21
8	15	7.37	20	19.70	35	55.49	45	227.21
9	20	16.75	25	41.21	25	84.23	45	214.20
10	15	17.73	25	43.92	35	60.05	30	159.60
11	20	15.67	25	44.12	30	74.52	40	225.46
12	15	18.34	30	34.50	35	61.19	45	241.95
13	15	14.00	20	29.00	30	63.81	35	167.96
14	15	34.16	20	73.82	25	99.49	35	203.96
15	15	2.61	20	13.18	40	34.55	45	198.55
16	20	26.68	25	57.95	35	95.56	20	236.72
17	10	0.21	15	0.53	10	0.04	40	31.87
18	15	5.40	25	11.24	30	27.78	25	49.82
19	15	3.99	25	19.27	30	28.89	40	91.68
20	15	4.75	20	11.89	25	18.82	40	57.25
21	10	4.42	20	8.64	35	21.09	35	56.05
22	10	0.62	10	0.62	10	0.10	10	1.90

TABLE 1 Cont'd

23	15	18.22	25	54.50	30	109.53	30	402.37
24a	15	21.47	30	65.56	30	108.77	30	274.27

TIME= Time needed to reach equilibrium conditions.

TABLE 2

ENTRAINMENT RATE AT SAMPLE SITES FOR EACH
APPLIED EFFECTIVE SHEAR STRESS

STATION	2 DYNE TEST (g/m ² /sec)	3 DYNE TEST (g/m ² /sec)	4 DYNE TEST (g/m ² /sec)	5 DYNE TEST (g/m ² /sec)
1	0.007	0.007	0.009	0.037
2	0.010	0.017	0.013	0.065
4	0.002	0.003	0.003	0.010
5	0.010	0.009	0.007	0.012
6	0.001	0.005	0.007	0.017
8	0.006	0.007	0.018	0.041
9	0.011	0.008	0.029	0.054
10	0.003	0.033	0.016	0.043
11	0.014	0.010	0.021	0.054
12	0.015	0.013	0.017	0.260
13	0.009	0.015	0.019	0.051
14	0.039	0.027	0.043	0.051
15	0.003	0.005	0.008	0.047
16	0.017	0.020	0.015	0.048
17	0.000	-	0.001	0.005
18	0.004	0.006	0.022	0.019
19	0.003	0.009	0.005	0.029
20	0.003	0.003	0.003	0.011

TABLE 2 Continued

21	0.003	0.004	0.002	0.010
22	0.001	0.001	0.000	0.003
23	0.016	0.020	0.025	0.161
24a	0.021	0.018	0.021	0.053

TABLE 3

PERCENT WATER CONTENT FOR SEDIMENTS AT EACH OF THE SAMPLE SITES

STATION	AVG. WATER CONTENT (%)	REPLICATE A (%)	REPLICATE B (%)	DIFFERENCE (%)
1	67.9	65.8	70.0	4.2
2	39.7	39.7	-	-
3	22.2	22.9	21.6	1.3
4	18.0	18.1	18.0	0.1
5	38.5	39.7	37.3	2.4
6	40.5	40.4	40.6	0.2
8	40.2	39.0	41.3	2.3
9	55.6	56.1	55.1	1.0
10	40.6	39.5	41.8	2.3
11	64.4	63.6	65.3	1.7
12	83.7	83.4	84.1	0.7
13	73.7	73.5	74.0	0.5
14	52.4	52.1	52.8	0.7
15	26.3	28.3	24.4	3.9
16	70.2	68.4	72.0	3.6
17	20.5	20.2	20.8	0.6
18	70.3	69.9	70.8	0.9
19	50.7	51.5	49.9	1.6
20	24.5	23.8	25.2	1.4

TABLE 3 Cont'd

21	33.1	32.8	33.5	0.7
21a	29.1	29.1	-	-
22	15.0	14.7	15.4	0.7
23	53.2	53.6	52.9	0.7
24a	55.2	54.8	55.9	1.1

TABLE 4 - Summary Sediment Properties for Sample Sites

Site:	Location:	Depth (Ft).	Sediment Type	Sediment Color	Mean Grain Size (ϕ)	Median Grain Size (ϕ)	Variance (ϕ)	Std. Dev.
1	West Pass-Mid	23	med. clayey slt	ol.gray	5.90	5.90	38.12	6.17
2	East Pass-Lo	75	v.fine silty sand	ol.gray	3.50	2.75	16.69	4.08
3	East Pass-Mouth	96	grav.silty sand	ol.gray	3.70	2.70	20.47	4.52
4	East Pass-Mouth	98	medium sand	ol.gray	1.70	1.25	5.48	2.34
5	East Pass-Lo	101	v.fine silty sand	ol.gray	4.30	3.70	21.55	4.64
6	East Pass-Mid	72	v.fine silty sand	ol.gray	4.30	3.80	22.43	4.74
8	East Pass-Mid	52	v.fine silty sand	ol.gray	4.20	3.70	23.25	4.82
9	East Passage-Mid	47	v.fine silty sand	ol.gray	4.60	4.70	29.71	5.45
10	Mt. Hope Bay	57	coarse sandy silt	ol.gray	4.80	5.00	29.35	5.42
11	Mt. Hope Bay	21	fine clayey silt	ol.black	5.90	6.20	37.99	6.16
12	Bristol Harbor	22	fine clayey silt	ol.gray	6.20	6.50	41.96	6.48
13	Warren R.-Mouth	21	med. clayey silt	ol.gray	5.80	5.80	37.30	6.11
14	Prov. River	43	v.fine silty sand	ol.gray	3.90	3.20	20.71	4.55
15	Prov. River	43	sand	ol.black	2.30	1.00	14.34	3.79
16	Ohio Ledge	22	medium clayey slt	ol.gray	5.30	5.80	35.52	5.96
17	West Pass-Up	18	medium sand	brwn gry	1.40	1.15	3.37	1.84
18	West Pass-Mid	32	fine clayey silt	ol.gray	5.80	6.20	38.44	6.20
19	West Pass-Mid	29	v.fine silty sand	ol.gray	4.30	3.65	22.61	4.75
20	West Pass-Lo	33	v.fine silty sand	ol.gray	3.50	2.95	14.66	3.83
21	West Pass-Lo	64	v.fine silty sand	ol.gray	4.30	3.95	24.52	4.95
21a	West Pass-Lo	64	v.fine silty sand	ol.gray	4.10	3.60	18.72	4.33
22	Sak Pass-Mouth	40	medium sand	ol.gray	1.80	1.50	4.49	2.12
23	Sak Pass-Mid	36	medium clayey slt	ol.gray	5.90	6.00	37.93	6.16
24a	Sak Pass-Up	30	medium clayey slt	ol.gray	5.80	6.00	37.02	6.08

Table 4. Cont'd

Site	Location	Skewness	Kurtosis	Mode	% Sand	% Silt	% Clay	Sand/slt Ratio	Slt/clay Ratio	Avg. Water Content (%)
1	West Pass-Mid.	1.34	1.34	4.0	5.5	73.1	21.4	0.1	3.42	67.9
2	East Pass-Lo	1.51	2.68	3.0	78.1	13.8	8.1	5.7	1.70	39.7
3	East Pass-Mth	1.50	2.49	2.5	66.6	19.7	13.7	3.4	1.44	22.2
4	East Pass-Mth	2.19	6.40	2.0	93.9	3.7	2.4	25.4	1.54	18.0
5	East Pass-Lo	1.24	1.74	4.0	60.1	34.9	5.0	1.7	6.98	38.6
6	East Pass-Mid	1.26	1.81	4.0	57.9	32.7	9.4	1.8	3.48	40.5
8	East Pass-Mid	1.34	1.99	3.0	54.2	34.3	11.5	1.6	2.98	40.2
9	East Pass-Mid	1.27	1.75	4.0	42.3	39.6	18.1	1.0	3.42	55.6
10	Mt. Hope Bay	1.27	1.74	5.5	35.6	51.6	12.8	0.7	4.03	40.7
11	Mt. Hope Bay	1.14	1.36	9.0	15.2	64.7	20.1	0.2	3.22	64.5
12	Bristol Harbr	1.11	1.30	4.5	7.2	65.9	26.9	0.1	2.45	83.7
13	Warren River	1.17	1.46	4.0	18.2	49.7	32.1	0.4	1.55	73.7
14	Prov. River	1.39	2.19	3.0	65.1	24.8	10.1	2.6	2.46	52.4
15	Prov. River	1.90	3.91	0.5	74.3	15.6	10.1	4.8	1.54	30.0
16	Ohio Ledge	1.21	1.54	9.0	23.6	54.8	21.6	0.4	2.54	70.2
17	West Pass-Up	1.81	4.78	1.5	98.3	1.4	0.3	70.2	4.67	20.5
18	West Pass-Mid	1.13	1.33	7.0	12.7	67.5	19.8	0.2	3.41	70.4
19	West Pass-Mid	1.31	1.92	4.0	56.2	33.9	9.9	1.7	3.42	50.7
20	West Pass-Lo	1.31	2.03	3.0	78.1	17.8	4.1	4.4	4.34	24.5
21	West Pass-Lo	1.32	1.90	3.0	50.4	40.3	9.3	1.3	4.33	33.2
21a	West Pass-Lo	1.20	1.64	4.0	64.2	31.7	4.1	2.0	7.73	29.1
22	Sak Pass-Mth	1.64	3.87	2.0	95.5	4.2	0.3	22.7	14.00	15.0
23	Sak Pass-Mid	1.12	1.33	4.0	11.7	69.2	19.1	0.2	3.62	53.2
24a	Sak Pass-Up	1.13	1.33	5.5	8.2	71.7	20.1	0.1	3.57	55.3

TABLE 5

Results of Method of Moments Calculations

Site	1st Moment (=mean grain size) (ϕ)	2nd Moment (variance)	Std. Dev. (sorting)	3rd Moment	Skew	4th Moment	Kurtosis
1	5.9 (medium silt)	38.12	6.17 (ext. poorly sorted)	264.41	1.12	1949.27	1.34
2	3.5 (v. fine sand)	16.69	4.08 (ext. poorly sorted)	103.05	1.51	747.00	2.68
3	3.7 (v. fine sand)	20.47	4.52 (ext. poorly sorted)	138.57	1.50	1044.63	2.49
4	1.7 (medium sand)	5.48	2.34 (v. poorly sorted)	28.11	2.19	192.41	6.40
5	4.3 (coarse silt)	21.55	4.64 (ext. poorly sorted)	123.81	1.24	809.00	1.74
6	4.3 (coarse silt)	22.43	4.74 (ext. poorly sorted)	143.32	1.26	910.00	1.81
8	4.2 (coarse silt)	23.25	4.82 (ext. poorly sorted)	150.11	1.34	1077.00	1.99
9	4.7 (coarse silt)	29.71	5.45 (ext. poorly sorted)	206.06	1.27	1542.00	1.75
10	4.8 (coarse silt)	29.35	5.42 (ext. poorly sorted)	202.00	1.27	1498.00	1.74
11	5.9 (medium silt)	37.99	6.16 (ext. poorly sorted)	266.00	1.14	1965.00	1.36
12	6.2 (fine silt)	41.96	6.48 (ext. poorly sorted)	302.00	1.11	2288.00	1.30
13	5.8 (medium silt)	37.30	6.11 (ext. poorly sorted)	266.00	1.17	2027.00	1.46
14	3.9 (v. fine sand)	20.71	4.55 (ext. poorly sorted)	131.00	1.39	937.00	2.19
15	2.3 (fine sand)	14.34	3.79 (v. poorly sorted)	103.00	1.90	803.00	3.91
16	5.3 (medium silt)	35.52	5.96 (ext. poorly sorted)	255.52	1.21	1938.00	1.54
17	1.4 (medium sand)	3.37	1.84 (poorly sorted)	11.21	1.81	54.00	4.78
18	5.8 (medium silt)	38.44	6.20 (ext. poorly sorted)	268.14	1.13	1962.00	1.33
19	4.3 (coarse silt)	22.61	4.75 (ext. poorly sorted)	140.55	1.31	981.90	1.92
20	3.5 (v. fine sand)	14.66	3.83 (v. poorly sorted)	73.55	1.31	436.00	2.03
21	4.3 (coarse silt)	24.52	4.94 (ext. poorly sorted)	159.74	1.32	1141.00	1.90
21a	4.1 (coarse silt)	18.72	4.33 (ext. poorly sorted)	97.26	1.20	575.00	1.64
22	1.8 (medium sand)	4.49	2.12 (v. poorly sorted)	15.58	1.64	78.00	3.87
23	5.9 (medium silt)	37.93	6.16 (ext. poorly sorted)	262.09	1.12	1915.00	1.33
24a	5.8 (medium silt)	37.02	6.08 (ext. poorly sorted)	253.48	1.13	1829.00	1.33

TABLE 6

SUMMARY OF CORRELATION ANALYSIS FOR SAMPLE SITES
FROM DATA OBTAINED FROM SEDIMENT ANALYSES

	ERATE2	ERATE3	ERATE4	ERATE5
DEPTH	(a) -0.12583 (b) 0.6550 (c) 15	-0.13799 0.6380 14	-0.13669 0.6271 15	-0.23785 0.3933 15
MNGR	0.66510 0.0068 15	0.50632 0.0647 14	0.65937 0.0075 15	0.59142 0.0202 15
MEDGR	0.67948 0.0053 15	0.55121 0.0410 14	0.69640 0.0039 15	0.61205 0.0153 15
VAR	0.68045 0.0052 15	0.52653 0.0531 14	0.70743 0.0032 15	0.62227 0.0132 15
SD	0.64563 0.0093 15	0.52526 0.0538 14	0.69086 0.0043 15	0.58328 0.0225 15
SKEW	-0.51681 0.0485 15	-0.3571 0.2094 14	-0.50735 0.0535 15	-0.42906 0.1105 15
KURT	-0.49591 0.0601 15	-0.37341 0.1885 14	-0.51551 0.0492 15	-0.41568 0.1233 15
SORT	0.64563 0.0093 15	0.52526 0.0538 14	0.69086 0.0043 15	0.58328 0.0225 15
MODE	0.56966 0.0266 15	0.73134 0.0030 14	0.59995 0.0181 15	0.39146 0.1490 15
PSAND	-0.67652 0.0056 15	-0.50524 0.0653 14	-0.66185 0.0072 15	-0.60157 0.0177 15

PSILT	0.65974 0.0074 15	0.50731 0.0641 14	0.61583 0.0145 15	0.57747 0.0242 15
PCLAY	0.69370 0.0041 15	0.46320 0.0953 14	0.77935 0.0006 15	0.64807 0.0090 15
SSLT	-0.43796 0.1025 15	-0.42370 0.1311 14	-0.46405 0.0814 15	-0.35543 0.1936 15
SLTCLY	-0.23727 0.3945 15	-0.25965 0.3700 14	-0.41100 0.1280 15	-0.31472 0.2532 15
PWATER	0.62830 0.0121 15	0.38790 0.1705 14	0.66954 0.0063 15	0.55209 0.0328 15

where: a= correlation coefficient,
 b= probability of finding a larger correlation
 coefficient,
 c= number of samples used in the analysis,
 ERATE2= entrainment rate at 2 dynes/cm²,
 ERATE3= entrainment rate at 3 dynes/cm²,
 ERATE4= entrainment rate at 4 dynes/cm²,
 ERATE5= entrainment rate at 5 dynes/cm²,
 MNGR= mean grain size,
 MEDGR= median grain size,
 VAR= variance,
 SD= standard deviation,
 SKEW= skewness,
 KURT= kurtosis,
 SORT= sorting,
 MODE= mode,
 PSAND= percent sand content,
 PSILT= percent silt content,
 PCLAY= percent clay content,
 SSLT= sand/silt ratio,
 SLT/CLY= silt/clay ratio,
 PWATER= percent water content.

TABLE 7

SUMMARY OF MEASURED VS PREDICTED ENTRAINMENT RATES
FOR SELECTED SAMPLE SITES

SITE	ERATE2		ERATE3		ERATE4		ERATE5	
	MEAS.	PRED.	MEAS.	PRED.	MEAS.	PRED.	MEAS.	PRED.
	(g/m ² /sec)		(g/m ² /sec)		(g/m ² /sec)		(g/m ² /sec)	
1	0.007	0.008	0.007	0.005	0.009	0.011	0.037	0.058
2	0.010	0.009	0.017	0.008	0.013	0.016	0.065	0.052
4	0.002	0.002	0.003	0.005	0.003	0.003	0.010	0.002
5	0.010	0.006	0.009	0.012	0.007	0.004	0.012	0.012
6	0.001	0.007	0.005	0.011	0.007	0.011	0.017	0.031
8	0.006	0.004	0.007	0.004	0.018	0.009	0.041	0.036
9	0.011	0.009	0.008	0.016	0.029	0.028	0.054	0.074
10	0.003	0.006	0.033	0.026	0.016	0.017	0.043	0.013
17	0.000	0.000	-	0.000	0.001	0.000	0.005	0.005
19	0.003	0.005	0.009	0.008	0.005	0.006	0.029	0.002
20	0.003	0.002	0.003	0.002	0.003	0.003	0.011	0.024
21	0.003	0.003	0.004	0.008	0.002	0.008	0.010	0.038
22	0.001	0.001	0.001	0.000	0.000	0.000	0.003	0.009
23	0.016	0.019	0.020	0.016	0.025	0.025	0.161	0.131
24a	0.021	0.016	0.018	0.022	0.021	0.019	0.053	0.063

ERATE2= Entrainment rate at 2 dynes/cm²ERATE3= Entrainment rate at 3 dynes/cm²ERATE4= Entrainment rate at 4 dynes/cm²ERATE5= Entrainment rate at 5 dynes/cm²

TABLE 8

SUMMARY OF MEASURED VS. PREDICTED ENTRAINMENT RATES FOR ALL
SAMPLE SITES

SITE	ERATE @ 2 dynes/cm ²		ERATE @ 3 dynes/cm ²		ERATE @ 4 dynes/cm ²		ERATE @ 5 dynes/cm ²	
	meas.	pred.	meas.	pred.	meas.	pred.	meas.	pred.
	(g/m ² /sec)		(g/m ² /sec)		(g/m ² /sec)		(g/m ² /sec)	
1	0.007	0.009	0.007	0.005	0.009	0.012	0.037	0.059
2	0.010	0.009	0.017	0.008	0.013	0.016	0.065	0.053
3	-	0.036	-	0.025	-	0.038	-	0.186
4	0.002	0.002	0.003	0.004	0.003	0.003	0.010	0.002
5	0.010	0.006	0.009	0.012	0.007	0.004	0.012	0.013
6	0.001	0.008	0.005	0.011	0.007	0.011	0.017	0.032
8	0.006	0.004	0.007	0.004	0.018	0.009	0.041	0.037
9	0.011	0.002	0.008	0.018	0.029	0.022	0.054	0.036
10	0.003	0.006	0.033	0.026	0.016	0.017	0.043	0.013
11	0.014	0.042	0.010	0.065	0.021	0.051	0.054	0.106
12	0.015	0.022	0.013	0.017	0.017	0.041	0.260	0.155
13	0.009	0.027	0.015	0.010	0.019	0.046	0.051	0.190
14	0.039	0.024	0.027	0.059	0.043	0.042	0.051	0.014
15	0.003	0.009	0.005	0.005	0.008	0.009	0.047	0.032
16	0.017	0.018	0.020	0.047	0.015	0.011	0.059	0.082
17	0.000	0.000	-	0.000	0.001	0.001	0.005	0.005
18	0.004	0.021	0.006	0.040	0.022	0.034	0.019	0.059
19	0.003	0.005	0.009	0.008	0.005	0.006	0.029	0.002
20	0.003	0.002	0.003	0.002	0.003	0.003	0.011	0.024
21	0.003	0.003	0.004	0.008	0.002	0.008	0.010	0.038
21a	-	0.000	-	0.003	-	0.003	-	0.006
22	0.001	0.001	0.001	0.000	0.000	0.000	0.003	0.009
23	0.016	0.019	0.020	0.017	0.025	0.025	0.161	0.132
24a	0.021	0.016	0.018	0.022	0.021	0.020	0.053	0.063

APPENDIX I

SEDIMENT SAMPLING LOCATIONS NOV. 21 - 28 1988 NARRAGANSETT BAY, RI

STATION	LAT.	LONG.	DEPTH (FT.)	SED. TYPE	DEVICE	LOCATION
1	41 35.50N	71 22.09W	23	CLAYEY SILT	GRAB	MIDBAY
2	41 31.68N	71 21.04W	75	SILTY SAND	GRAB	LOWER BAY
3	41 27.77N	71 22.10W	96	GRAV. SAND	GRAB	EAST PASSAGE
4	41 27.49N	71 22.74W	98	SAND	BOX/GRAB	EAST PASSAGE
5	41 31.44N	71 20.06W	101	SILTY SAND	BOX/GRAB	LOWER BAY
6	41 32.50N	71 19.91W	72	SILTY SAND	BOX/GRAB	LOWER BAY
8	41 36.52N	71 17.32W	52	SILTY SAND	BOX/GRAB	MIDBAY
9	41 37.42N	71 17.69W	47	SILTY SAND	BOX/GRAB	MIDBAY
10	41 38.90N	71 14.50W	57	SANDY SILT	BOX/GRAB	MT.HOPE BAY
11	41 41.55N	71 12.83W	21	CLAYEY SILT	BOX/GRAB	MT.HOPE BAY
12	41 40.09N	71 17.22W	22	CLAYEY SILT	BOX/GRAB	BRISTOL HARBOR
13	41 41.60N	71 18.07W	21	CLAYEY SILT	BOX/GRAB	RUMSTICK NECK
14	41 45.74N	71 22.57W	43	SILTY SAND	GRAB	PROV. RIVER
15	41 48.75N	71 23.89W	43	SAND	GRAB	PROV. RIVER
16	41 41.83N	71 20.15W	22	CLAYEY SILT	BOX/GRAB	UPPER BAY
17	41 39.13N	71 23.12W	18	SAND	BOX/GRAB	UPPER BAY
18	41 37.86N	71 23.23W	32	CLAYEY SILT	BOX	MIDBAY
19	41 33.59N	71 24.59W	29	SILTY SAND	BOX/GRAB	MIDBAY
20	41 32.76N	71 24.55W	33	SAND	GRAB	LOWER BAY
21	41 30.19N	71 24.85W	64	SILTY SAND	BOX/GRAB	LOWER BAY
21A	41 26.79N	71 24.72W	51	SILTY SAND	BOX/GRAB	WEST PASSAGE
22	41 29.40N	71 13.06W	40	SAND	BOX	SAKONNET RIVER
23	41 34.17N	71 13.32W	36	CLAYEY SILT	BOX/GRAB	SAKONNET RIVER
24A	41 35.37N	71 13.23W	30	CLAYEY SILT	GRAB	SAKONNET RIVER

APPENDIX II

DETERMINATION OF SILT AND CLAY CONTENT USING PIPETTE ANALYSIS

1. A subsample representative of the sediments in the grab sampler was taken that yielded between 5-15 g of silt and clay-size sediment.
2. Samples were placed in 50 ml beakers in a solution of distilled water and hydrogen peroxide and allowed to remain until they were disaggregated. A rubber tipped stirring rod or spatula was used to further break up the sample gently.
3. The disaggregated sample was wet-sieved through a 4 phi (0.063-mm) sieve. The fine material (i.e. silts and clays) was collected in an underlying evaporating dish.
4. The material on the sieve (i.e. <.063 mm fraction) was transferred to another beaker for use in the determination of sand content. This material was oven dried and weighed to the nearest 0.001 g.
5. The less than 63 mm fraction which was collected in the evaporating dish was transferred to a graduated one (1) liter glass column.
6. Dispersant ("Calgon") was added to the cylinder to prevent flocculation of the clay fraction. Approximately 0.051 g of Calgon was added to each column.
7. The column was filled to the 1000 ml mark and thoroughly stirred.
8. The column was stored for 12 hours. This is done to observe if flocculation of the clay fraction has occurred. If so, repeat steps 6-8, accounting for the weight of the additional dispersant. If not, proceed to step 9.
9. After approximately twelve hours, the column was thoroughly stirred and a pipette with depth gradations was used to withdraw 20 ml aliquots at the calculated times and depth intervals. Withdrawal times were determined based on water temperature, measured by thermometer, at the beginning of the experiment. Samples were withdrawn at 0.5 phi (~.010 mm) intervals between 4.0 phi (.063 mm) and 9.0 phi (.002 mm).
10. The pipetted material was placed into individual beakers and, when completed, all beakers were placed in an oven at 100-130°C for approximately 24 hrs. to dry.

APPENDIX II Cont'd

11. After drying, the beakers were removed from the oven and left to cool for at least 1.5 hrs. (this allows the clay fraction to equilibrate with the humidity in the room). The beakers were weighed to the nearest .001 g and their weights recorded.

12. The weight of the sediment from the 4 phi sample was multiplied by 50 and the weight of the dispersant subtracted to give the total weight of the mud (F). This value was then added to the weight of the sand (S; see Step 4) to give the total weight of the sample. The quantity obtained by multiplying each later pipette sample (4.5 phi, 5.0 phi etc.) by 50 is (P).

13. Cumulative weight percentages were then determined by substituting the above values into the following formula:

$$\text{Cumulative Percent} = 100 (S+F-P) / S+F$$

Coarser

where S= weight of sand

F= weight of mud (silt + clay)

P= weight of each size fraction

14. These values were then plotted on cumulative curves which are available upon request.

APPENDIX III

DETERMINATION OF SAND CONTENT BY SIEVING TECHNIQUES

The procedure for the sieve size analysis of sand is as follows:

1. The greater than 4 phi fraction (>0.063 mm) was processed and dried during the separation of the sand fraction from the mud fraction for pipette analysis. This material was then poured through 8 in. diameter screens nested according to decreasing diameter and increasing phi size. The sieves were arranged at 0.5 phi (~ 0.010 mm) intervals between -0.5 phi (1.4 mm) and 4.0 phi (.063 mm).
2. The screens were placed in a shaker device (i.e. a Ro-Tap) and sieved (or shaken) for 15 min.
3. The material from each sieve or size fraction was placed in a tared pan and weighed.
4. Each fraction was then examined under a binocular microscope to estimate the percentage of aggregates in the sample. This is done by counting 100 grains. This percentage is subtracted from the sample weight.
5. Cumulative percent was determined by dividing the total cumulative weight by the weight of each size fraction times 100.
6. These values were then plotted on cumulative curves and are available upon request.

APPENDIX IV

DETERMINATION OF WATER CONTENT FROM SEDIMENT SAMPLES

The procedure for the determination of water content of surficial sediments is presented below. Water content is derived relative to the wet weight of the sediment and results in values between 1-99%. In contrast, water content derived relative to the dry weight of sediment may result in values greater than 100% for sediments primarily composed of silts and clays.

1. Cores collected for % water content were sealed and frozen to prevent water loss through evaporation and leakage prior to analysis.
2. The cores were later thawed to room temperature. The thawing procedure was conducted with the core sealed to prevent water loss during this process. The length of time involved was long enough to allow the perimeter of the core to be unfrozen from its plexiglas lining but not of such duration to completely unthaw the sediment sample. This procedure is necessary to break the bond between the sample and the side of the core tube which results from the freezing process.
3. The top and bottom of the cores were unsealed. A circular plexiglas "plunger", with a diameter equal to the inside of the core liner, was used to extrude the surficial section approximately 1.5 - 2.0 inches above the plexiglas top of the liner.
4. The upper 5 mm of the core top was divided in half using perpendicular and lateral cuts with a razor blade. This results in a working section and an archive section.
5. The working section was then halved and the two sections were placed into tared beakers and weighed to obtain the "wet" weight. This allows for conducting replicate analyses on the sediment samples.
6. The working sections were then oven dried for approximately 24 hours at 100°C and placed in a dessicator for cooling.
7. Sections from other cores were handled according to the above methodology and those beakers were subsequently weighed to obtain a "dry" weight.
8. The following formula was used to determine results:
$$\% \text{ Water Content} = 100 (\text{"wet" weight} - \text{"dry" weight}) / \text{"wet" weight}$$

Appendix V

DETERMINATION OF SEDIMENT ERODIBILITY USING THE PARTICLE ENTRAINMENT SIMULATOR (PES)

Introduction

The PES is a portable device designed to apply a shear stress to a sediment surface (Fig. 1). An acrylic tube with intact or packed sediment and seawater is placed in the PES so that a perforated grid oscillates vertically in water above the sediment surface. The resuspension potential of that sediment is assessed by measuring suspended solids concentration with respect to time and converting values to mass flux ($\text{g/m}^2/\text{time}$).

Oscillation-shear relationship

Previous experiments were performed using the PES and an annular flume to develop a quantitative relationship between oscillation rate, flume rotational speed and suspended solids concentration at equilibrium or steady state conditions (Tsai and Lick, 1986). The oscillation rate associated with the PES and the sediments concentration that was suspended were compared with a known rotational shear rate in the annular flume and resulting suspended solids concentrations. Equivalent shear stresses were identified when equal suspended solids concentrations were produced in both the annular flume and the PES for a standard sediment at a known shear stress.

Benthic shear in an annular flume was calibrated by the particle velocity method, using a laser doppler velocimeter, to determine rotational speeds producing shear values between $2\text{--}12 \text{ dynes/cm}^2$.

Those rates are (Fig. 2):

Oscillation Rate	Equivalent Flume Shear
0.16(00) sec/oscillation	2 dynes/cm ² (extrapol.)
0.12(00)	3 dynes/cm ²
0.10(00)	4 "
0.08(00)	5 "

PES Apparatus Installation (shipboard or lab bench)

Alignment

The alignment of the PES requires that (1) the rod supporting the grid be perpendicular to a flat surface (e.g. a lab table), (2) the PES be firmly anchored to minimize any vibration, and (3) lubricant be regularly applied to protect the PES from mechanical wear. A large carpenter square is used to initially check the vertical alignment of the PES. It is very important for the PES to be secured and properly aligned.

Test Core Set-up procedure

The sediment core is placed with a restraining rubber band into a glass dish on four clay "pads". The purpose of the glass dish is to capture fluid should the core leak or in the event of catastrophic loss. The dish and sediment core are carefully lifted so that the oscillating grid enters the acrylic tube with no sample disturbance. When dish is in place, a lab jack is inserted under dish to provide stability.

This assembly is raised until the bottom side of grid is exactly 2.0" above the sediment/water interface, when grid is at its lowest level.

The water column above the sediment is adjusted to a height of 5.0" above mean level of the sediment/water interface and that level marked. Test runs are then begun at lowest shear value of interest.

Light attenuation measurement

The Bausch & Lomb Spec-20 is presently used to measure light transmission (which is later converted to light attenuation or extinction coefficient). The wave length window is set at 660 nm. The Spec-20 is calibrated with 3 clean test tubes (3 ml), each filled with deionized water. These tubes continue to serve as references for re-calibration during the course of the experiment.

Experimental Test

Start-up: Initially, the sediment core is slowly mixed at 0.6-0.7 sec/oscillation (for approximately 1 minute) to gently mix the water column without resuspending sediment. The suspended solids concentration (derived from light attenuation) is measured and is labelled time zero SSC. The oscillation rate is steadily increased to 0.16 sec/osc, at which timing of the experiment begins. Light transmission is monitored at set time intervals until steady state or near- steady state conditions are reached:

Time (min)

0 (prior to start of test)

1

2

3

4
5
10
15
20

and at 5-10 minute intervals until (near) steady state is reached (Fig. 3).

Criteria for steady state are (1) less than 2 % point change in light transmission during a 5 minute period, and (2) a minimal test run of:

15 minutes for a 2 dyne/cm ² test	
20	3
25	4
30	5

When steady state is judged, the sample is checked on the spectrophotometer and the final light attenuation value serves as the time zero value for the next shear test (Fig. 4). The grid oscillation rate is then increased to next shear test.

When testing highly unstable sediment the Spec-20 will saturate (approaching 0% transmission), thus providing both uncertain values (too sensitive) and insufficient data (part of curve missing). One simple approach to handle this problem is to dilute the sample (e.g. 1:10), measure transmission, calculate the suspended solids concentration, and finally to multiply that value by 10 to compute the final value.

Calculations

The PES data set is comprised of a series of light transmission data as a function of time, usually between 0 and 30-60 minutes. These values are converted to suspended solids concentration according to:

$$SS = [(-1/k_1) * (\ln k_2 - LA/k_3)]^{1/k_2}$$

where $k_1 = 1.5092$

$k_2 = 0.9527$

$k_3 = 99.9432$

LA = % light attenuated.

SS = Suspended solids concentration (mg/l)

The suspended solids concentration (mg/l) for each applied stress was then converted to grams/meter² (i.e. mass flux) by multiplying by the chamber volume (1.347 l) and dividing by the sediment surface area (108 cm²).

Lavelle and Davis (1987) indicate that the suspended solids concentration time series can also be used to calculate entrainment rate using:

$$E = \alpha_1 * h / (1 - C_0 / \alpha_2)$$

where E = Entrainment rate

h = height of the fluid column

α_1 = the time rate of change for the entrainment rate

C_0 = initial concentration @ t=0

α_2 = equilibrium concentration

if the initial concentration at the start of each stress test, its time rate of change, and the equilibrium concentration are known.

Quality Assurance

The PES is not in wide application and therefore must be considered an experimental prototype.

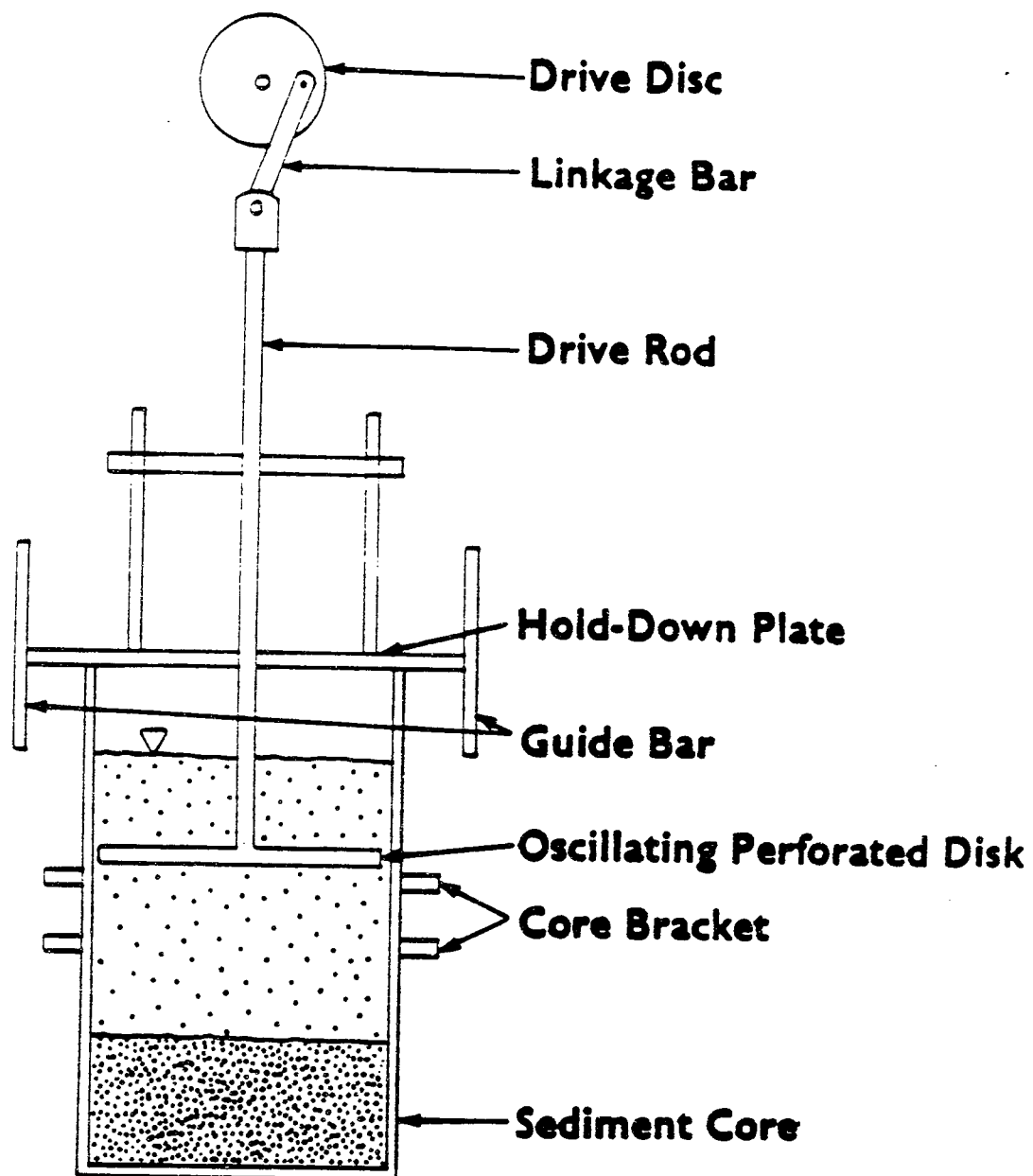


Fig. 1- Schematic diagram of the Particle Entrainment Simulator
(from Tsai and Lick, 1986).

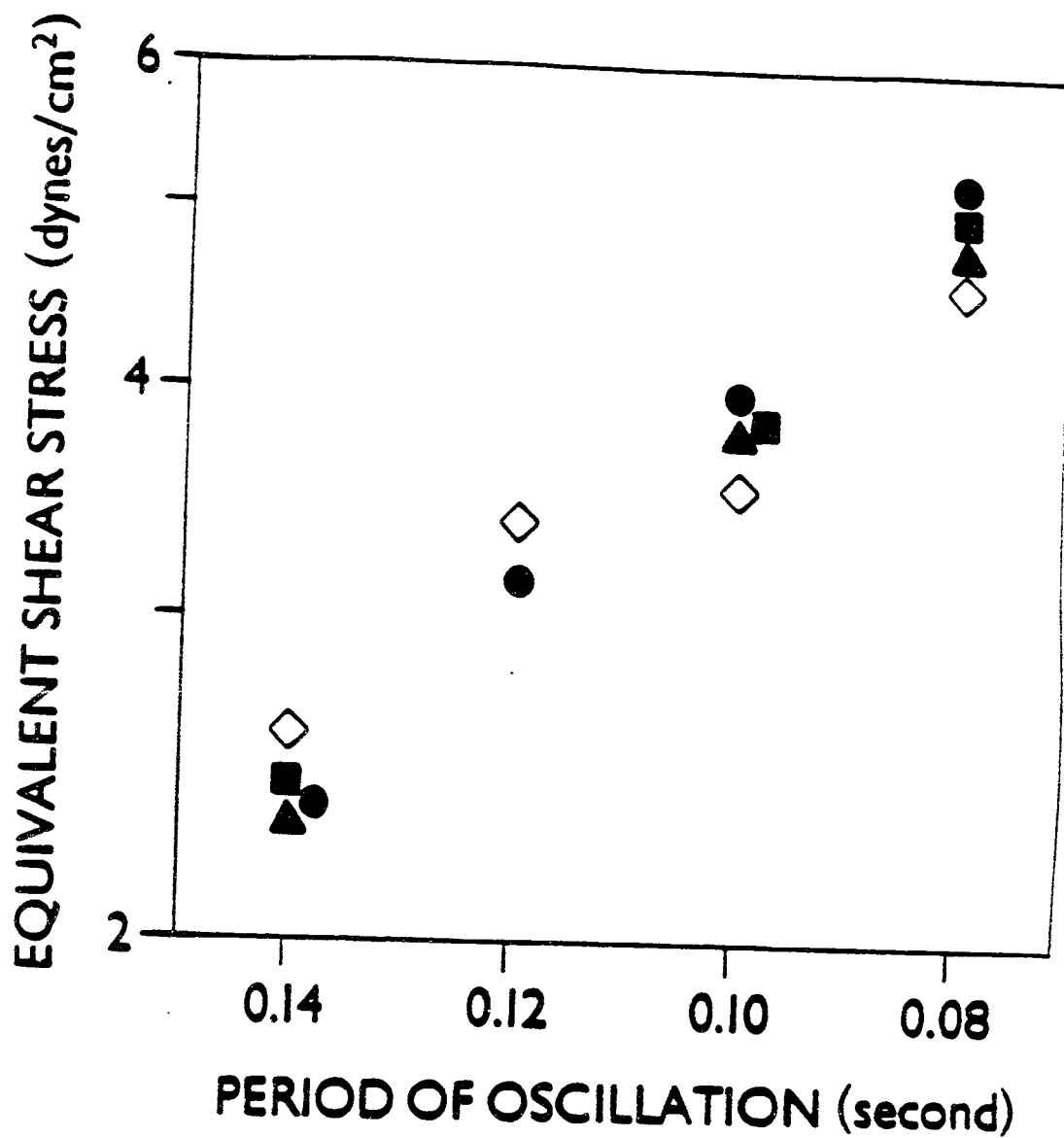


Fig. 2- Empirical relationship between disk oscillation frequency and equivalent bottom stress from Tsai and Lick (1986). Closed and open symbols represent two and seven days consolidation of sediment prior to experiments.

Fig. 3- Example plots of suspended solids concentration vs. time.

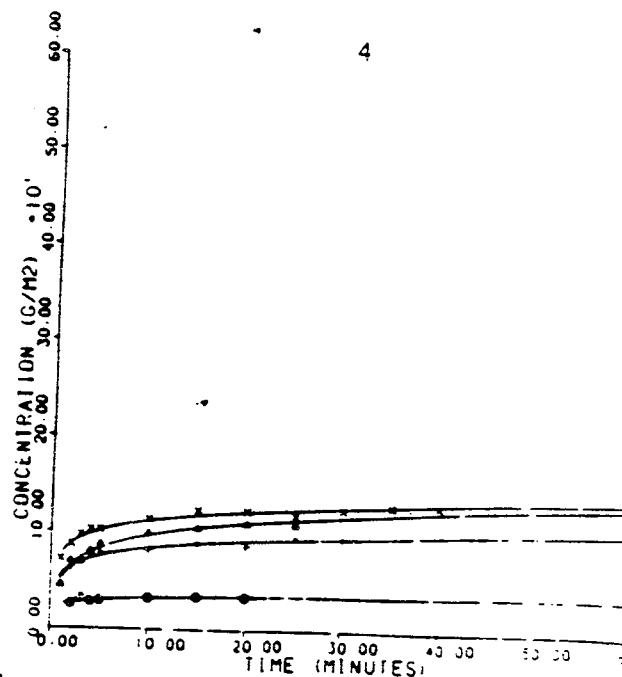
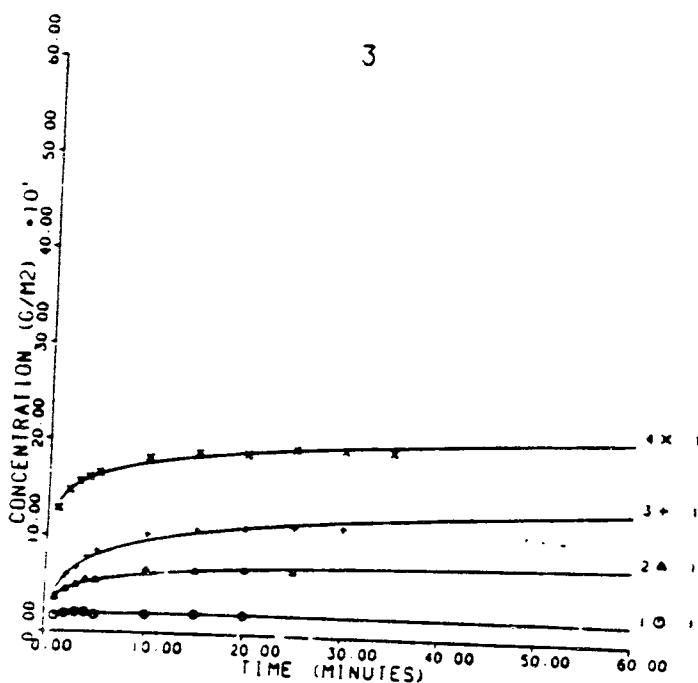
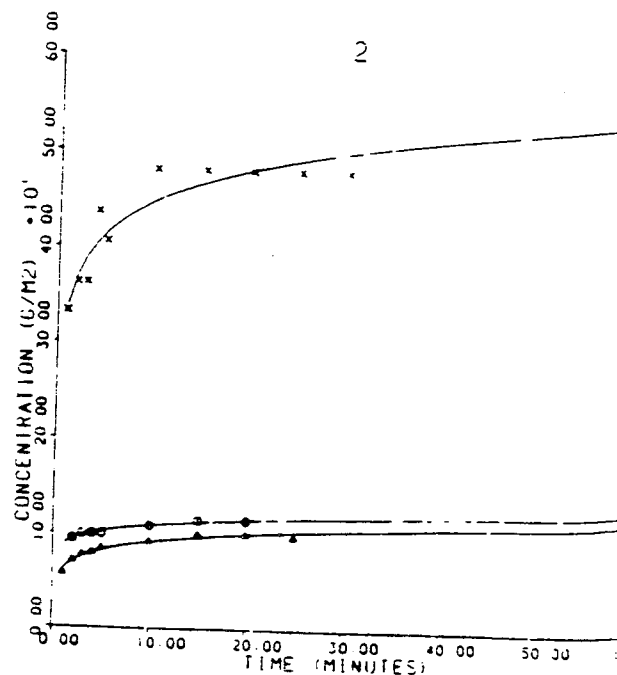
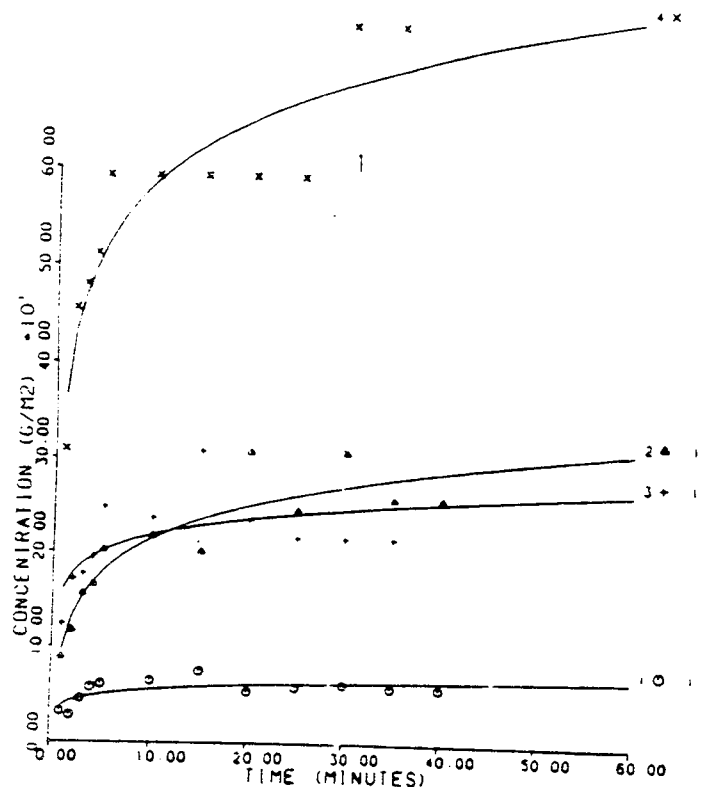


Fig. 4- Time series of light attenuation - suspended solids concentration from Lavelle and Davis, 1987.

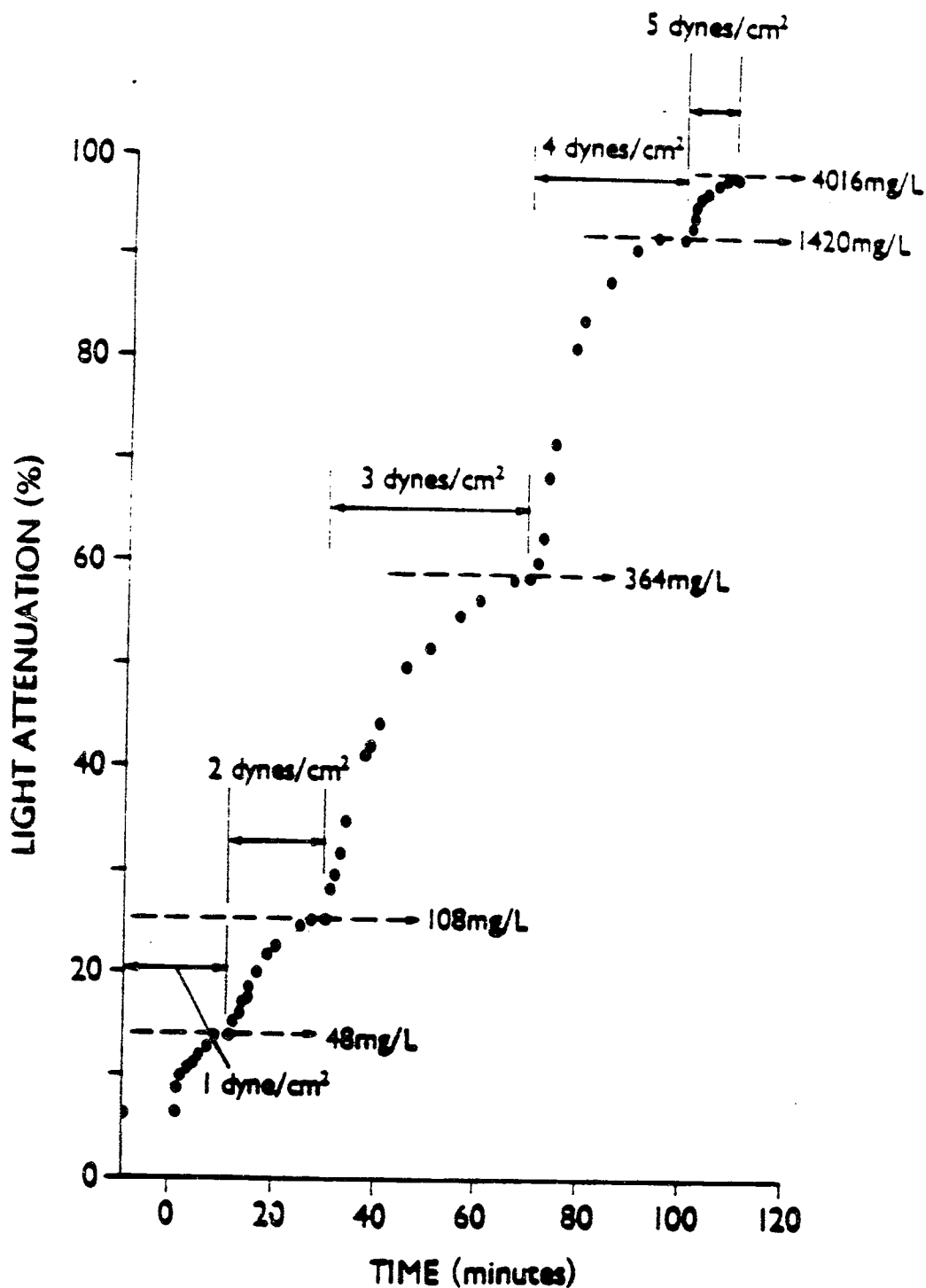


Figure Time series of light attenuation in subsamples drawn from the entrainment chamber over intervals of constant equivalent bottom stress. Data comes from the Shilshole-central core.